

Expanding the Therapeutic Potential of the Iron Chelator Deferasirox in the Development of Aqueous Stable Ti(IV) Anticancer Complexes

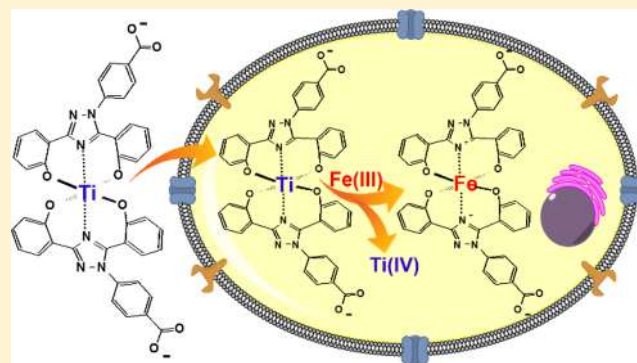
Sergio A. Loza-Rosas,[†] Alexandra M. Vázquez-Salgado,[†] Kennett I. Rivero,[†] Lenny J. Negrón,[†] Yamixa Delgado,[†] Josué A. Benjamín-Rivera,[†] Angel L. Vázquez-Maldonado,[†] Timothy B. Parks,[‡] Charlene Munet-Colón,[†] and Arthur D. Tinoco*,[†] 

[†]Department of Chemistry, University of Puerto Rico, Río Piedras Campus, Río Piedras, Puerto Rico 00931, United States

[‡]VA Caribbean Healthcare System, 10 Casia Street, San Juan, Puerto Rico 00921, United States

Supporting Information

ABSTRACT: The recent X-ray structure of titanium(IV)-bound human serum transferrin (STf) exhibiting citrate as a synergistic anion reveals a difference in Ti(IV) coordination versus iron(III), the metal endogenously delivered by the protein to cells. This finding enriches our bioinspired drug design strategy for Ti(IV)-based anticancer therapeutics, which applies a family of Fe(III) chelators termed chemical transferrin mimetic (cTfm) ligands to inhibit Fe bioavailability in cancer cells. Deferasirox, a drug used for iron overload disease, is a cTfm ligand that models STf coordination to Fe(III), favoring Fe(III) binding versus Ti(IV). This metal affinity preference drives deferasirox to facilitate the release of cytotoxic Ti(IV) intracellularly in exchange for Fe(III). An aqueous speciation study performed by potentiometric titration from pH 4 to 8 with micromolar levels of Ti(IV) deferasirox at a 1:2 ratio reveals exclusively $[\text{Ti}(\text{deferasirox})_2]^{2-}$ in solution. The predominant complex at pH 7.4, $[\text{Ti}(\text{deferasirox})_2]^{2-}$, exhibits the one of the highest aqueous stabilities observed for a potent cytotoxic Ti(IV) species, demonstrating little dissociation even after 1 month in cell culture media. UV-vis and ¹H NMR studies show that the stability is unaffected by the presence of biomolecular Ti(IV) binders such as citrate, STf, and albumin, which have been shown to induce dissociation or regulate cellular uptake and can alter the activity of other antiproliferative Ti(IV) complexes. Kinetic studies on $[\text{Ti}(\text{deferasirox})_2]^{2-}$ transmetalation with Fe(III) show that a labile Fe(III) source is required to induce this process. The initial step of this process occurs on the time scale of minutes, and equilibrium for the complete transmetalation is reached on a time scale of hours to a day. This work reveals a mechanism to deliver Ti(IV) compounds into cells and trigger Ti(IV) release by a labile Fe(III) species. Cellular studies including other cTfm ligands confirm the Fe(III) depletion mechanism of these compounds and show their ability to induce early and late apoptosis.



INTRODUCTION

In recent years, efforts to make Ti(IV) compounds viable anticancer agents have surged. They demonstrate outstanding promise because of their wide spectrum of activity and lack of cross-resistance with platinum-based anticancer drugs,^{1–5} one of the major classes of commercial drugs in the market. Ever since the lead Ti(IV) compounds, budotitane and titanocene dichloride, did not advance far in clinical trials due to low efficacy,^{4,6,7} different strategies have been developed to design more potent compounds.

The research groups of Tacke, Meléndez, McGowan, Gomez-Ruiz, Kaluderovic, and Baird have synthesized second-generation titanocene complexes to overcome the major limitations of the parent compound: namely, poor water solubility and instability due to extensive hydrolysis.⁸ Modifications made include substitutions with less labile ligands and with ligands that allow for higher cellular specificity and biocompatibility.^{9–21} McGowan and Lord have also

synthesized and characterized a library of second-generation budotitane complexes.²² They showed improved solubility, aqueous stability up to 2 weeks, and increasing cytotoxicity upon addition of electron-withdrawing substituents to the β -diketonate ligand. The researchers Tshuva and Huhn have taken a different approach in Ti(IV) drug development by introducing other classes of ligands: the tetradentate diamino bis(phenolato) (salan) and *N,N'*-ethylenebis(salicylimine) (salen) ligands. Ti(IV) complexes of these ligands are significantly more soluble, stable in solution, and cytotoxic.^{23–26}

They are generally six-coordinate with alkoxide ligands satisfying the remainder of the coordination sites. Recently Huhn prepared a heptacoordinate version of these compounds with the tridentate 2,6-pyridinedicarboxylate ligand (Ti(salan)-(dipic)) to further improve solution stability.²⁷

Received: February 28, 2017

While significant advances have been made in the design of Ti(IV) anticancer complexes, there are still limitations with these complexes. For instance, *in vivo* studies demonstrate that some of these complexes, despite improved stability, have low tumor accumulation.²⁸ Another limitation of Ti(IV) complexes is the sparse understanding of their mechanism of action, which prevents a smart design of ligands for enhanced activity. Most of the ligands used merely function as stabilizing delivery vehicles for the Ti(IV). The ligands, however, have far more potential in being actively involved in the cytotoxicity of the complexes. By better understanding the solution behavior of Ti(IV) under physiological conditions and its elusive biochemistry, ligands can be selected and engineered to facilitate the metal's cytotoxic properties.

Our recent insight into the mechanism of Ti(IV) transport in the human body²⁹ has helped us develop a novel Ti(IV)-based anticancer drug design approach. Serum transferrin (STf), the iron(III) blood transport protein, works in synergy with the small anion citrate to stabilize Ti(IV) in serum, transport it into cells, and regulate its activity so that it is not toxic to the cells²⁹ and might be able to participate in cellular functions. The crystal structure for STf coordination of Ti(IV) reveals an interesting and unusual binding in which Ti(IV) is coordinated by two of the four protein amino acids that typically coordinate Fe(III), the two tyrosines, and citrate in place of the histidine and aspartate residues (Figure 1).²⁹

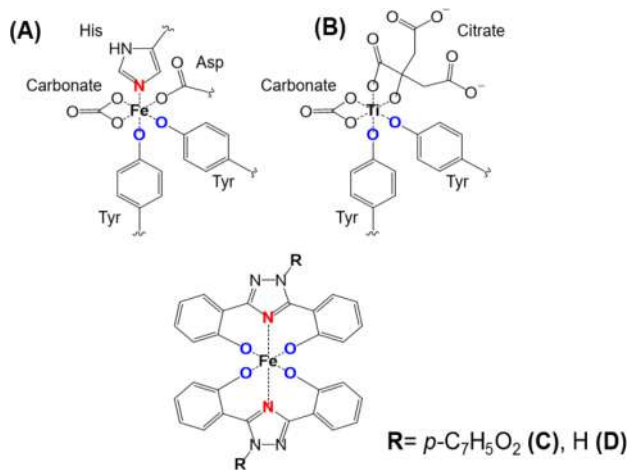


Figure 1. (A) STf Fe(III) binding site consisting of two Tyr, one His, and one Asp residue. The synergistic anion carbonate satisfies the remaining coordination sites. (B) STf Ti(IV) binding site consisting of the citrate anion coordinating the metal in place of His and Asp and serving as a synergistic anion. (C, D) Tridentate chemical transferrin mimetic (cTfm) ligands (C) deferasirox and (D) 3,5-bis(2-hydroxyphenyl)-1,2,4-triazole (BHPT) providing moieties that favor Fe(III) binding in a manner comparable to STf binding.

The differences between Fe(III) and Ti(IV) STf binding suggest a difference in metal affinity, with the four protein amino acids combined having a higher affinity for Fe(III) than for Ti(IV). The STf metal binding site is thus a template for ligand design, one to exploit the differences in Fe(III) and Ti(IV) affinity in an anticancer approach. Since cancer cells have a significantly higher requirement for iron than normal cells,³⁰ lowering the bioavailability and overall levels of this essential metal would be detrimental to these cells. A promising direction in anticancer drug development is targeting the molecular mechanisms that keep cancer cells alive.³¹ There is

increased attention to the use of iron chelators such as desferrioxamine, triapine, and thiosemicarbazones for these purposes, showing promising antiproliferative properties *in vitro* and *in vivo* against different types of tumors.^{32–34} Inspired by the metal binding site of STf as a classical Fe(III) chelator, we apply a new family of small molecules called chemical transferrin mimetic ligands (cTfm) for the development of Ti(IV) anticancer complexes.³⁵ The ligands mimic STf coordination of Fe(III) in order to favor Fe(III) binding versus Ti(IV). This metal binding preference would facilitate a two-pronged method of attack. Ti(IV) release is triggered by cTfm binding of Fe(III). The Ti(IV) then attacks intracellular target sites and the bioavailable Fe(III) pool is decreased, both processes causing harm to the cells (Figure 2). The Ti(IV)-STf-citrate structure helps to identify specific cTfm ligands that could effectively accomplish our proposed strategy.

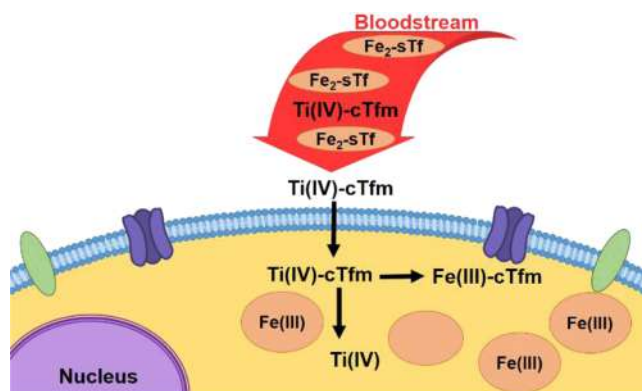


Figure 2. cTfm strategy, where the cTfm ligands release Ti(IV) and then capture Fe(III) via a transmetalation process in cancer cells. The cytotoxic effect combines the decrease in bioavailable Fe with Ti(IV) binding to intracellular targets.

In this work we explore the use of deferasirox (4-[3,5-bis(2-hydroxyphenyl)-1,2,4-triazole-1-yl]benzoic acid), an FDA-approved iron chelator,³⁶ as a cTfm ligand to regulate and enhance Ti(IV) cytotoxicity. The structure of deferasirox (Figure 1) exhibits a central triazole core coupled to two phenol substituents that mimics the His and Tyr residues present in the STf metal binding site. This structure mimics STf Fe(III) coordination moieties. The ligand has a higher affinity for Fe(III) ($\log \beta = 36.9$)³⁷ in comparison with any other metal studied.³⁸ Due to its iron chelation capacity, deferasirox is already being actively investigated for its potential as an anticancer therapeutic.³⁹ Deferasirox binding of Ti(IV) is explored in the solid and solution state via multiple spectroscopic techniques. Where necessary, the structural analogue 2-[3-(2-hydroxyphenyl)-1H-1,2,4-triazol-5-yl]phenol (BHPT) is used for characterization purposes. These characterizations provide the speciation insight needed to understand the general aqueous stability of the Ti(IV) deferasirox complex in order to identify the dominant species in the physiological pH range of 4.3–7.4. By examining how key serum biomolecules, which are known to bind Ti(IV) in ion and/or compound form, can affect the cytotoxicity of Ti(IV) compounds being developed for anticancer purposes, we identify structural properties that are important for Ti(IV) compounds to maximize their potency. This information is used to assess whether Ti(IV) deferasirox can survive bloodstream conditions. We also examine the effectiveness of

deferasirox to deliver Ti(IV) to cells and to facilitate its activity intracellularly due to its Fe(III) affinity preference. The intracellular feasibility is explored by performing deferasirox transmetalation experiments using physiologically relevant Fe(III) sources. Our bioinspired drug design strategy reveals how ligand metal affinity preference can be fine-tuned to regulate metal-based cytotoxicity.

EXPERIMENTAL SECTION

Materials. All aqueous solutions were prepared with autoclaved (121 °C and 18 psi) high-quality nanopure water (18.2 MΩ cm resistivity, Thermoscientific Easypure water purifier). 4-[*(3Z,SE)-3,5-Bis(6-oxocyclohexa-2,4-dien-1-ylidene)-1,2,4-triazolidin-1-yl]benzoic acid (deferasirox) was purchased from Focus Synthesis LCC (San Diego, CA). 2-[3-(2-Hydroxyphenyl)-1*H*-1,2,4-triazol-5-yl]phenol (BHPT) was purchased from Princeton Biomolecular Research Inc. (Princeton, NJ). Potassium dioxalatooxotitanate(IV) dihydrate ($K_2[TiO(C_2O_4)_2] \cdot 2H_2O$) and citratoiron(III) ($Fe(C_6H_5O_7)$) were obtained from Sigma-Aldrich. Dicitratoiron(III), $[Fe(citrate)_2]^{5-}$ ($Fe(C_6H_5O_7)_2^{5-}$), was prepared *in situ* by mixing equimolar amounts of $Fe(C_6H_5O_7)$ and citrate in solution and adjusting the pH to 7.4.³⁵ $[Fe(deferasirox)_2]^{3-}$ and $[Fe(BHPT)_2]^{2-}$ were prepared *in situ* by mixing 1 equiv of $FeCl_3$ (dissolved in 10 mM HCl) with 2 equiv of deferasirox and BHPT (both dissolved in DMF), respectively.³⁷ Both complex solutions were adjusted to pH 7.4. For the determination of pK_a values, high-purity 0.01 M NaOH (carbonate-free) solution was purchased (Fisher Chemical). A549 human lung cancer cells and MRCS human lung normal cells were obtained from ATCC (CCL-185 and CCL-171, respectively). Both cell lines were cultured in phenol red DMEM (Sigma, D6429) containing 1% of glutamine and 4.5 g/mL of glucose and sodium pyruvate and supplemented with 10% FBS (HyClone) and 1% of antibiotic solution prepared with 11 mg/mL streptomycin and 7 mg/mL penicillin (Calbiochem, EMD Biosciences Inc.) at 37 °C in a humidified atmosphere of 5% (v/v) CO_2 . Phenol Red free DMEM (CellGro REF 17–205-CV) was used during cytotoxicity studies. 3-(4,5-Dimethylthiazol-2-yl)-2,5-diphenyltetrazolium bromide (MTT) was purchased from EMD Biosciences Inc. (La Jolla, CA). The CellTiter 96 aqueous nonradioactive cell proliferation assay kit was purchased from Promega (Madison, WI). The Alexa Fluor 488 Annexin V/Dead Cell Apoptosis Kit was obtained from ThermoFisher (Waltham, MA). Human apo-transferrin (Sigma, T2036) and bovine serum albumin (Amresco, 0332) were used during the stability studies of Ti(IV) in aqueous solution. A Microsep advance centrifugal device (Pall Corp., 3K MWCO) was used for rapid spin dialysis of bovine serum albumin, while human apo-transferrin was dialyzed using regenerated cellulose dialysis tubing 3.5K MWCO (Fisher Scientific, 21-152-9). MALDI TOF/TOF was performed using a matrix composed of 6-aza-2-thiothymine (Fluka, 82393) and 3-hydroxycoumarin (Aldrich, 642673).*

Instruments. A Cary 300 UV-vis spectrophotometer was used for kinetics experiments. All pH values were determined by using a Thermoscientific Orion Star A211 and an Orion 9157BNMD electrode, calibrated with standard buffer solutions at pH 4, 7, and 10. For the determination of pK_a values, a Thermoscientific Orion Star A211 and Ross ultra refillable triode electrode, 8157BNUMD (Thermoscientific), were used. The electrode was calibrated before each titration in units of mV. Solutions of pH 0–4 and 10–14 were prepared to graph pH as a function of mV. The Nernst equation ($E = E_0 - k \times T \times pH$) was used to convert mV to pH. The titration glass vessel was thermostated by attaching it to a water bath (Isotemp, Fisher Scientific). A Büchi R-200 rotovapor and Eppendorf 5702 centrifuge were used for all synthetic protocols. FT-IR spectra were collected on a Nicolet iS50 FT-IR spectrometer. Mass spectra were collected on a MALDI TOF/TOF AB SCIEX 4800 Analyzer and a Waters Micromass Q-TOF with electrospray ionization (ESI) at a capillary voltage of 3000 and sample cone voltage of 30. 1H NMR solution spectra were recorded on a Bruker 500 MHz instrument typically in a 50/50 d_6 -DMSO/ D_2O mixture at 25 °C. Multiwell plate absorbance was measured in a Multiskan FC, Thermoscientific plate

reader. Cells were grown in a Revco Elite III RCO5000T-5-ABC incubator. Cell counting and culture viability monitoring were performed using a Nikon Eclipse TS-100 microscope. Confocal microscopy studies were performed using a Nikon Ti-E inverted microscope with A1R confocal microscopes. X-ray diffraction data were collected at $T = 296 \pm 2$ K with a Bruker APEX-2 CCD diffractometer with graphite-monochromated Mo $K\alpha$ radiation ($\lambda = 0.71073 \text{ \AA}$). Cyclic voltammetry was performed with a Princeton Applied Research Parstat 2273 advanced electrochemical system using Powersuite software. The counter electrode was a platinum wire. An Ag/AgCl saturated electrode was used as reference. A glassy-carbon electrode of 2 mm diameter was used as a working electrode.

Synthesis of $Ti(C_{42}H_{26}N_6O_8) \cdot 0.5H_2O$ ($Ti(deferasirox)_2$, mol wt 826.595). A 100 mg portion (0.3 mmol) of deferasirox was dissolved in 10 mL of methanol, and 48 mg (0.1 mmol) of $K_2[TiO(C_2O_4)_2] \cdot 2H_2O$ was dissolved in 5 mL of water. Both colorless solutions were mixed and stirred for 1 h. The yellow precipitate product was obtained by centrifugation to remove any soluble material over 20 min at 4400 rpm. It was washed by resuspending in water and centrifuging, and this process was repeated three times. The product was dried under vacuum and then stored at room temperature and protected from light (yield 91%). CHN elemental analysis was performed by Atlantic Microlabs (Norcross, GA). Anal. Calcd (found): C, 63.01 (63.09); H, 3.44 (3.40); N, 10.40 (10.51). UV-vis (H_2O , DMSO 5%): pH 4.3, λ_{max} 370 nm, $\epsilon = 11100 \text{ M}^{-1} \text{ cm}^{-1}$ (proposed to be $Ti(deferasirox)_2$, $Ti(C_{42}H_{26}N_6O_8)$); pH 7.4, λ_{max} 365 nm ($\epsilon = 11332 \text{ M}^{-1} \text{ cm}^{-1}$) (proposed to be $[Ti(deferasirox)]^{2-}$; $Ti(C_{42}H_{24}N_6O_8)^{2-}$). FT-IR data (cm^{-1}): $\nu(C=O)$ 1701; $\nu(C-O)$ 1272, 1261; $\nu(Ti-O)$ 860. Mass spectrum (positive ion mode, MALDI TOF/TOF): $[Ti(C_{42}H_{24}N_6O_8)]^{2-} + 3H^+$, m/z 791.573. The matrix was composed of a 1/1 mixture of 10 mg/mL of 6-aza-2-thiothymine and 10 mg/mL of 3-hydroxycoumarin. Both matrix solutions were prepared in a solvent composed of acetonitrile and water in a 1/1 ratio.⁴⁰ 1H NMR (ppm): 6.26 (t); 6.67 (t); 6.95 (t); 7.01 (d); 7.20 (m); 8.06 (d); 8.19 (d); 8.25 (d). 1H NMR (ppm) of metal-free ligand: 6.89 (d); 7.01 (m); 7.39 (q); 7.56 (d); 8.0 (d); 8.06 (d); 10.5 (s); 10.8 (s). The reduction potentials of $Ti(deferasirox)_2$ at pH 4.3 ($E^\circ = -0.839 \text{ V}$ vs NHE) and pH 7.4 ($E^\circ = -0.905 \text{ V}$ vs NHE) were measured by cyclic voltammetry. Conditions: 1 mM $[Ti(deferasirox)_2]^{2-}$, 0.1 M KNO_3 , glassy-carbon working electrode, Ag/AgCl reference electrode, scan rate 25 mV/s.

Synthesis of $Ti(C_{28}H_{18}N_6O_4) \cdot C_3H_6O_2 \cdot H_2O$ ($Ti(BHPT)_2$, mol wt 644.46). A 102 mg portion (0.3 mmol) of BHPT was dissolved in 10 mL of DMF, and 70 mg (0.1 mmol) of $K_2[TiO(C_2O_4)_2] \cdot 2H_2O$ was dissolved in 5 mL of water. The solutions were mixed for 1 h. The orange precipitate product was obtained by centrifugation to remove any soluble material over 20 min at 4400 rpm. It was washed by resuspending in water and centrifuging, and this process was repeated three times. The product was dried under vacuum and then stored at room temperature and protected from light (yield 87%). Anal. Calcd (found): C, 57.83 (57.77); H, 4.67 (4.37); N, 12.99 (13.04). UV-vis (H_2O , DMSO 5%): pH 4.3, λ_{max} 416 nm, $\epsilon = 16467 \text{ M}^{-1} \text{ cm}^{-1}$ (proposed to be $Ti(BHPT)_2$, $Ti(C_{28}H_{18}N_6O_4)$); pH 7.4, λ_{max} 415 nm ($\epsilon = 16217 \text{ M}^{-1} \text{ cm}^{-1}$) (proposed to be $[Ti(BHPT)]^{2-}$; $Ti(C_{28}H_{16}N_6O_4)^{2-}$). FT-IR data (cm^{-1}): $\nu(C-O)$ 1261; $\nu(Ti-O)$ 871. Mass spectrum (positive ion mode, MALDI TOF/TOF): $[Ti(C_{28}H_{16}N_6O_4)]^{2-} + 3H^+$, m/z 551.095. The matrix was composed of a 1/1 mixture of 10 mg/mL 6-aza-2-thiothymine and 10 mg/mL of 3-hydroxycoumarin. Both matrix solutions were prepared in a solvent composed of acetonitrile and water in a 1/1 (v/v) ratio plus trifluoroacetic acid at 0.1% (v/v). 1H NMR (ppm): 6.38 (d); 6.95 (t); 7.25 (t); 8.19 (dd). 1H NMR (ppm) of metal-free ligand: 6.96 (q); 7.34 (t); 7.99 (dd).

Crystallization of $Ti(BHPT)_2$. A 0.5 mg portion (0.912 μmol) of $Ti(BHPT)_2$ was dissolved in 30 μL of DMF. The solution was mixed with 90 μL of diethyl ether. Crystals were obtained via air evaporation at room temperature after a period of 4 days.

Crystal Structure Determination of $Ti(BHPT)_2$. Crystal data: $C_{28}H_{18}N_6O_4Ti$, mol wt = 550.35, orange block, $0.39 \times 0.17 \times 0.14 \text{ mm}^3$, monoclinic, C2 (No. 5), $a = 19.613(4) \text{ \AA}$, $b = 8.9973(18) \text{ \AA}$, $c =$

$12.241(3)$ Å, $\beta = 119.586(2)^\circ$, $V = 1878.4(7)$ Å 3 , $Z = 2$, $\rho_{\text{calc}} = 0.97$ g cm $^{-3}$. X-ray diffraction data from a single crystal mounted atop a glass fiber were collected at $T = 296 \pm 2$ K with a Bruker APEX-2 CCD diffractometer with graphite-monochromated Mo $\text{K}\alpha$ radiation ($\lambda = 0.71073$ Å). Collected data were corrected for Lorentz and polarization effects. A multiscan absorption correction was applied using SADABS4 ($\mu = 0.260$ mm $^{-1}$, 0.948–0.964 correction range). The structure was solved with direct methods⁴¹ and refined by a Gauss–Newton method using the OLEX2 program.⁴² All non-hydrogen atoms were refined anisotropically. The hydrogen atom of the triazole group was located in the difference Fourier map and was kept fixed in the located position; all other hydrogen atoms were placed in calculated positions and refined with their thermal ellipsoids riding on the corresponding carbon atoms. Large solvent-accessible voids in the crystal structure of $\text{Ti}(\text{BHPT})_2$ are occupied by interstitial solvent molecules, whose crystallographic disorder could not be modeled satisfactorily. Consequently, the diffraction data set of $\text{Ti}(\text{BHPT})_2$ was modified by the Solvent Mask feature of the OLEX2 program before the final refinement. In all, 180 parameters were refined with 1 restraint. A total of 9084 reflections were collected up to $\theta_{\text{max}} = 25.010^\circ$; 3283 were unique ($R_{\text{int}} = 0.0183$). $R1 = 0.0342$ for 3166 independent reflections with $I > 2\sigma(I)$, $wR2 = 0.1014$ for all data. $S = 1.037$. Flack α parameter = 0.26(13). The residual electron density was between -0.16 and 0.04 e Å $^{-3}$.

Potentiometric Titration of $[\text{Ti}(\text{deferasirox})_2]^{2-}$ To Determine the pK_a of the Carboxylic Acid Moieties. All titrations were performed at 25 °C with stirring, and all titration solutions had an initial volume of 15.0 mL. A 333 μM stock solution of $[\text{Ti}(\text{deferasirox})_2]^{2-}$ was prepared in DMSO. The stock solution was diluted to start the titration at 100 μM of complex in 30% DMSO/70% 0.10 M KCl/H₂O. The KCl was used to maintain a constant ionic strength of 0.07 M. The solution was left to equilibrate for 30 min. Aliquots of 0.01 M NaOH were titrated into the solution by micropipet in volumes ranging from 10 to 20 μL. After the addition of each aliquot of base, the solutions were equilibrated for ~10 min, when the millivoltage reading remained constant for 1 min. This experiment was performed in triplicate. For the determination of the pK_a the software CurTiPot was used.

Stability Studies of $[\text{Ti}(\text{deferasirox})_2]^{2-}$ in Aqueous Solution and in the Presence of the Biomolecules Albumin, Tf, and Citrate at pH 7.4. The following set of reactions was performed in quadruplicate at 25 °C. A 50 μM solution of $[\text{Ti}(\text{deferasirox})_2]^{2-}$ was reacted with 0.1 and 5 mM citrate at pH 7.4 (0.1 M Tris buffer, 0.1 M NaCl) and also with no citrate during a period of up to 7 days. The stability of the complex was evaluated by monitoring any changes in its LMCT band ($\lambda = 365$ nm; $\epsilon = 11300$ M $^{-1}$ cm $^{-1}$) by UV-vis spectroscopy.

The aqueous stability of $[\text{Ti}(\text{deferasirox})_2]^{2-}$ and $[\text{Ti}(\text{BHPT})_2]^{2-}$ was also evaluated by monitoring any change in the ^1H NMR (Bruker 500 MHz, 128 scans per sample) spectra of the complexes at pH 3.9 and 7.0 (pH 4.3 and 7.4, respectively) during a period of 4 days. Complexes were dissolved first in d_6 -DMSO and then diluted to a 1/1 ratio with D₂O to a final concentration of 50 μM and 1.5 mL final volume. pH was adjusted using NaOD and DCl. Additional samples of $[\text{Ti}(\text{deferasirox})_2]^{2-}$ and $[\text{Ti}(\text{BHPT})_2]^{2-}$ at pH 7.0 were incubated at 37 °C and monitored through ^1H NMR during a period of 4 days (Bruker 500 MHz, 128 scans per sample).

A 50 μM solution of $[\text{Ti}(\text{deferasirox})_2]^{2-}$ was reacted with 25 μM apo-STf and 100 μM citrate at pH 7.4 (20 mM Hepes, 27 mM NaHCO₃, 0.1 M NaCl) during 72 h. At 24 h time intervals, an aliquot of the reaction was dialyzed extensively to remove unreacted material. STf binding of Ti(IV) was then determined by monitoring the formation of the $\text{Ti}_2\text{-STf-(CO}_3)_2\text{-citrate}_2$ complex ($\lambda = 321$ nm; $\epsilon = 10000$ M $^{-1}$ cm $^{-1}$) using UV-vis spectroscopy and also by quantifying the Ti(IV) content via the 2,3-dihydroxynaphthalene-6-sulfonate colorimetric assay.⁶

Four different concentrations of $[\text{Ti}(\text{deferasirox})_2]^{2-}$ (10, 30, 50, and 70 μM) were reacted with 45 μM apo-BSA at a final volume of 100 μL (20 mM Hepes, 0.1 M NaCl, pH 7.4). The reaction mixtures were left to equilibrate overnight. The samples were then washed to

remove any compound unbound to the protein using centrifugal filters. The final samples were concentrated to roughly the initial volume and quantified by a Bradford assay.⁴³ Binding of $[\text{Ti}(\text{deferasirox})_2]^{2-}$ was determined by monitoring its LMCT band and also by quantifying the Ti(IV) content via a 2,3-dihydroxynaphthalene-6-sulfonate colorimetric assay.²⁹

Deferasirox Transmetalation of Ti(IV) by Fe(III). The following set of reactions was performed in quadruplicate and at 25 °C. A 50 μM solution of $[\text{Ti}(\text{deferasirox})_2]^{2-}$ and 100 μM of metal-free ligand were reacted with 25 μM of Fe(III) saturated transferrin (Fe₂-STf) over the course of 72 h at pH 7.4 (20 mM Hepes, 27 mM NaHCO₃, 0.1 M NaCl). Fe₂-STf was prepared by reacting micromolar amounts of apo-STf with 4 mol equiv of $[\text{Fe}(\text{citrate})_2]^{5-}$ (mole ratio 1/2) in 20 mM Hepes buffer containing 0.1 M NaCl and 27 mM NaHCO₃ and dialyzing extensively. The Fe(III) content was determined by the ferrozine colorimetric assay⁴⁴ and by monitoring the Fe₂-STf-(CO₃)₂ LMCT band ($\lambda = 465$ nm; $\epsilon = 5200$ M $^{-1}$ cm $^{-1}$).²⁹ At 24 h time intervals, an aliquot of the reaction was dialyzed extensively. The protein content in the aliquots was determined by the Bradford assay,⁴³ and the Fe(III) content was determined by measuring the Fe₂-STf-(CO₃)₂ LMCT band.

A 50 μM solution of $[\text{Ti}(\text{deferasirox})_2]^{2-}$ was also reacted with 50 μM $[\text{Fe}(\text{citrate})_2]^{5-}$ at 25 °C. The reaction was followed by both UV-vis spectroscopy and a Waters Micromass Q-ToF spectrometer. In the UV-vis window of 325–650 nm the disappearance of the LMCT band for $[\text{Ti}(\text{deferasirox})_2]^{2-}$ was tracked in addition to the formation of the LMCT band for $[\text{Fe}(\text{deferasirox})_2]^{3-}$ ($\lambda = 420$ nm, $\epsilon = 5720$ M $^{-1}$ cm $^{-1}$; $\lambda = 477$ nm, $\epsilon = 4050$ M $^{-1}$ cm $^{-1}$).³⁷ The mass spectrometry data were collected in negative ion mode, using source and desolvation temperatures of 100 and 250 °C, respectively. The mass range was 300–1000 m/z. For the mass spectrometry experiments, the solutions were not prepared in the Hepes buffer but instead a 5 mM ammonium bicarbonate (NH₄HCO₃) volatile buffer (pH 7.4).

A 50 μM solution of $[\text{Ti}(\text{deferasirox})_2]^{2-}$ was reacted with different concentrations of $[\text{Fe}(\text{citrate})_2]^{5-}$ (0.05, 0.1, 0.15, 0.2, 0.3, 0.4, and 0.5 mM) in the presence of a high concentration of citrate (5 mM). The reactions were measured every 1 min for the first 10 min, then every 2 min up to the 60 min time point, and finally every 1 h up to the 12 h time point. The rate dependence of the formation of the product observed in the early time points of this reaction on $[\text{Fe}(\text{citrate})_2]^{5-}$ concentration was examined. A plot of absorbance at 510 nm versus time (min) at the early time points were fit using the equation

$$\text{Abs}_{510 \text{ nm}} = A + B(1 - e^{k_{\text{obs}}t}) \quad (1)$$

where A = initial absorbance, B = amplitude, and k_{obs} = observed rate constant (min $^{-1}$). The data were further analyzed as indicated in the Supporting Information.

Cytotoxicity Studies. A549 and MRC5 cytotoxicity by the compounds was evaluated by using the colorimetric 3-(4,5-dimethylthiazol-2-yl)-2,5-diphenyltetrazolium bromide (MTT) assay. Incubation conditions were the same in all of the steps. Cells >95% confluence (grown in 100 × 20 mm tissue culture dishes, BD Falcon) were separately seeded into 96-well plates using phenol red free DMEM (containing 10% FBS and 1% streptomycin/penicillin) in a volume of 100 μL at a concentration of 1.0×10^5 cells/mL for A549 and 2.0×10^5 cells/mL for MRC5. The cells were incubated for 24 h and then treated with deferasirox, $[\text{Ti}(\text{deferasirox})_2]^{2-}$, BHPT, and $[\text{Ti}(\text{BHPT})_2]^{2-}$. The metal-bound and metal-free ligands were prepared in PBS pH 7.4 immediately before addition to the cells. Stock solutions were first prepared in DMF and diluted to specific concentrations (0.5–80 μM $[\text{Ti}(\text{deferasirox})_2]^{2-}$; 1–160 μM deferasirox; 0.01–12.5 μM $[\text{Ti}(\text{BHPT})_2]^{2-}$; 0.09–100 μM BHPT) using PBS while DMF was maintained at 1% (v/v) for metal-bound and metal-free ligands (controls also contained the same percentage of DMF). A 100 μL portions of solutions were added in all cell-containing wells with four replicates per concentration. The final percentage of DMF was 0.5. The plates were incubated for 72 h. At 4 h before completion of the incubation time, 25 μL of MTT solution (sterile-filtered 4 mg/mL solution, diluted in PBS buffer) was added to

each well. During addition of the MTT solution, the plates were protected from light and were returned to the incubator for the remaining 4 h until a purple precipitate was visible. A 50 μ L portion of 24.42% (w/v) SDS solution (sterile-filtered) was added to each well and incubated for 12 h. The absorbance of each well was measured at 570 and 690 nm (as a reference wavelength). The IC₅₀ values with standard error of means were determined by nonlinear regression of a variable slope (four-parameter) model by GraphPad Prism6.0 software from dose-response curves.

In a related experiment, A549 and MRC5 cells were grown in 100 \times 20 mm tissue culture dishes (BD Falcon) until 50% confluence. Media were discarded and replaced with 10 mL of DMEM containing 1% DMF with and without 25 μ M [Ti(deferasirox)₂]²⁻, 80 μ M deferasirox, or 6 μ M BHPT. After 24 h, images of the treated cultures were taken using a Nikon Eclipse TS100 microscope with attached digital camera. The deferasirox treatment was performed on a separate day and another no treatment control experiment was included to directly compare with this sample.

To improve the solubility of Ti(BHPT)₂, stock solutions were prepared in DMF and diluted to specific concentrations (2–30 μ M) using Triton X-100, a detergent suitable for cell membrane permeabilization, dissolved at 0.1% (v/v) in PBS while DMF was maintained at 1% (v/v). Solutions (100 μ L portions) were incubated with A459 and MRC5 cells seeded in 96-well plates during 24 h. To determine the solubility improvement related to the use of 0.1% Triton X-100, stock solutions previously prepared were UV-vis scanned and a standard curve was plotted with concentration (μ M) against absorbance at 415 nm. Stock solutions aimed at 60 μ M ($N = 3$) were prepared and centrifuged to precipitate undissolved compound; absorbances of the supernatant at 415 nm were used to determine the concentration of the saturated solution of Ti(BHPT)₂ dissolved in PBS (pH 7.4, 0.1% Triton X-100, 1% DMF).

Stability/Cytotoxicity of Ti(IV) Compounds in Cell Culture Media. Stock solutions of 300 μ M [Ti(deferasirox)₂]²⁻, [Ti(OHBED)]⁻, and [Ti(BHPT)₂]²⁻ were prepared in 20 mM Hepes buffer (pH 7.4), but [Ti(OHBED)]⁻ and [Ti(BHPT)₂]²⁻ had to be first dissolved in DMSO and then mixed with the buffer. [Ti(OHBED)]⁻ contained 6% DMSO, and [Ti(BHPT)₂]²⁻ contained 33% DMSO. The stock solutions were incubated at 4, 24, and 37 °C for 30 days. On the 29th day, A549 cells were seeded at 5 \times 10⁴ cells/mL and 100 μ L was added into each well of a 96-well plate. Cells were incubated with a final concentration of 50 μ M [Ti(deferasirox)₂]²⁻ and [Ti(OHBED)]⁻ and 30 μ M of [Ti(BHPT)₂]²⁻ (final 3.3% DMSO) for 24 h. Next, the cell viability was measured using the *CellTiter 96 aqueous non-radioactive cell proliferation assay* (Promega). At 1 h before completion of the incubation time, 20 μ L of 3-(4,5-dimethylthiazol-2-yl)-5-(3-carboxymethoxyphenyl)-2-(4-sulfophenyl)-2H-tetrazolium, inner salt (MTS), and phenazine methosulfate (PMS) solution were added to each well (333 μ g/mL MTS + 25 μ M PMS) and incubated for 1 h at 37 °C. The absorbance of each well was measured at 492 nm in a Multiskan FC, Thermoscientific plate reader spectrophotometer. Note that the use of 3.3% DMSO was higher than that in other experiments in order to achieve higher concentrations of [Ti(BHPT)₂]²⁻. This percentage of DMSO could compromise the viability of the cells and was used only for these set of experiments and for early and late apoptosis assays.

Fe(III) Supplementation Cell Viability Experiment. A549 and MRC5 cells were incubated in 96-well plates, as indicated in the MTT assay described above. After the first 24 h of incubation, half of the cells were supplemented with 40, 100, and 150 μ M [Fe(citrate)₂]⁵⁻. The cells were incubated for an additional 2 h. They were then treated with buffer, 80 μ M deferasirox, 40 μ M [Ti(deferasirox)₂]²⁻, and 40 μ M [Fe(deferasirox)₂]³⁻ control. In a related experiment, A549 cells were supplemented with 40, 100, and 150 μ M [Fe(citrate)₂]⁵⁻ and treated with buffer, 10 μ M BHPT, 5 μ M [Ti(BHPT)₂]²⁻, and 5 μ M [Fe(BHPT)₂]²⁻ control. The final percentage of DMSO was maintained at 0.5. The MTT assay was performed with these samples. A Student *t* test was performed to evaluate the differences in all cell viabilities between treatment and no treatment with [Fe(citrate)₂]⁵⁻.

Early and Late Apoptosis. A549 and MRC5 cells were seeded at 5 \times 10⁴ cells/mL and 500 μ L per well was added into Lab-tek chambered coverslips (4 wells). A final concentration of 50 μ M of [Ti(deferasirox)₂]²⁻, deferasirox, [Ti(OHBED)]⁻, and HBED in 20 mM Hepes buffer (pH 7.4, 5 mM NaHCO₃) and 30 μ M concentrations of [Ti(BHPT)₂]²⁻ and BHPT in the same buffer with 3.3% of DMSO were added to cells for 24 h. Untreated cells incubated with just media and Hepes buffer were used as the control. For detection of early and late apoptosis, the medium was removed and the cells were washed with cold 1× PBS twice. We used the *Alexa Fluor 488 Annexin V/Dead Cell Apoptosis Kit* for the analysis. Cell were incubated with 10 μ L of the Annexin V conjugate and 2 μ L of the 100 μ g/mL propidium iodine (PI) solution into each 300 μ L of annexin-binding buffer at room temperature for 15 min protected from light. Cells were washed three times with 500 μ L of 1× PBS. Finally, cells were covered with glycerol, as a fluorescence preservative, for further confocal analysis. The treated coverslips were examined under a Nikon Ti-E inverted microscope with A1R confocal microscopes. For the analysis, Alexa Fluor was excited at 495 nm and its emission was detected at 519 nm. PI was excited at 488 nm and its emission detected above 505 nm.

RESULTS AND DISCUSSION

Structural Characterization of the Ti(IV) Complexes of deferasirox and BHPT in Solid State and Aqueous Solution. A major requirement for the selection of an iron chelator as a cTfm ligand is that it stably coordinates Ti(IV) in aqueous solution, preventing hydrolysis-induced metal dissociation at physiological pH. To this end a Ti(IV)-bound deferasirox complex was synthesized, maintaining the metal/ligand ratio of 1/2 in solution. This ratio is important in trying to accomplish the Ti(IV) coordination number preference of 6.^{45,46} A neutral form of the compound Ti(deferasirox)₂ (Ti[C₄₂H₂₆N₆O₈]) (see the *Experimental Section*) readily precipitates from aqueous solution. Dissolving this compound in water at millimolar concentrations requires a cosolvent such as DMF or DMSO. The compound easily dissolves in water at pH 7.4 (low millimolar concentrations, including minimum 1% v/v of cosolvent) due to the deprotonation of the benzoic acid moiety of the ligand. Needlelike crystals of the neutral compound were obtained by dissolving 0.15 mg (0.19 μ mol) of Ti(deferasirox)₂ in 540 μ L of a 1/1 chloroform/toluene mixture but were not of high X-ray diffraction quality. For insight into the structure of the compound, Ti(BHPT)₂ was synthesized with an elemental formulation of Ti[C₂₈H₁₈N₆O₄] (see the *Experimental Section*). This neutral compound is even less water soluble than Ti(deferasirox)₂ because of the absence of the benzoic acid moiety and requires a cosolvent such as DMF or DMSO to obtain micromolar concentrations. The X-ray structure of Ti(BHPT)₂ (*Figure 3*) reveals C₂ symmetry, where Ti(IV) is coordinated in a meridional fashion by the BHPT ligands. This coordination is comparable with Fe(III) coordination by a BHPT derivative, which includes a 1-phenyl substituent on the triazole ring.³⁷

In both the Ti(IV) and Fe(III) structures, the N atoms from the two coordinated BHPT ligands are trans to one another. The phenol oxygen atoms on each ligand are coordinated trans to one another. Due to the bite restriction, the O–Ti–O angle is 162.68°, similar to the O–Fe–O angle (166.5°),³⁷ deviating from 180° (*Table 1*). The N–Ti–N angle of 177.92(11)° is much closer to ideal relative to the N–Fe–N angle of 172.7(3)°.³⁷ The difference in bond angles has to do with the Ti–N bond lengths (2.1450(15) Å) being longer than the Fe–N bond lengths (2.092(5) Å) and the Ti–O bond lengths (1.887(9) Å) being shorter than the Fe–O bond lengths (1.98

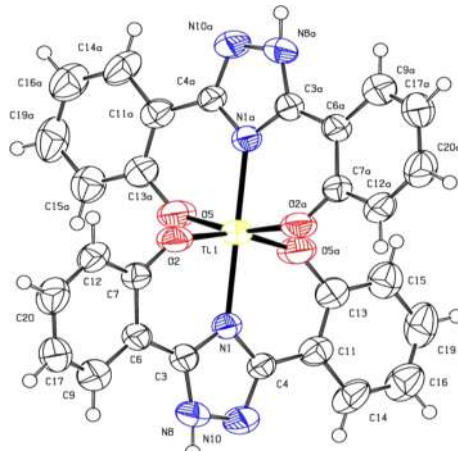


Figure 3. ORTEP diagram of $\text{Ti}(\text{BHPT})_2$. Unhydrolyzed $\text{Ti}(\text{IV})$ is coordinated by the tridentate ligand BHPT in a 1/2 molar ratio. This compound models the $\text{Ti}(\text{IV})$ coordination by deferasirox.

Table 1. Bond Distances (\AA) and Angles (deg) of $\text{Ti}(\text{BHPT})_2$ with Standard Uncertainties in Parentheses^a

Ti1—N1	2.1450(15)	C6—C7	1.425(3)
Ti1—N1 ⁱ	2.1450(15)	C6—C9	1.443(3)
Ti1—O2 ⁱ	1.8939(17)	C7—C12	1.410(3)
Ti1—O2	1.8939(17)	N8—N10	1.336(3)
Ti1—O5	1.8818(18)	C9—C17	1.332(4)
Ti1—O5 ⁱ	1.8818(18)	C11—C13	1.385(3)
N1—C3	1.353(3)	C11—C14	1.398(3)
N1—C4	1.367(3)	C12—C20	1.385(4)
O2—C7	1.294(3)	C13—C15	1.390(3)
C3—C6	1.437(3)	C14—C16	1.391(4)
C3—N8	1.335(3)	C15—C19	1.388(4)
C4—N10	1.327(3)	C16—C19	1.369(5)
C4—C11	1.480 (3)	C17—C20	1.378(4)
O5—C13 ⁱ	1.322(3)		
N1—Ti1—N1 ⁱ	177.92(11)	C11—C4—N10	124.04(19)
O2—Ti1—N1	82.09(7)	C13 ⁱ —O5—Ti1	143.30(16)
O2 ⁱ —Ti1—N1 ⁱ	82.09(7)	C7—C6—C3	118.9(2)
O2—Ti1—N1 ⁱ	99.39(7)	C9—C6—C3	122.6(2)
O2 ⁱ —Ti1—N1	99.39(7)	C9—C6—C7	118.2(2)
O2 ⁱ —Ti1—O2	90.11(11)	C6—C7—O2	122.0(2)
O5—Ti1—N1	97.91(7)	C12—C7—O2	119.97(19)
O5 ⁱ —Ti1—N1 ⁱ	97.91(7)	C12—C7—C6	117.9(2)
O5—Ti1—N1 ⁱ	80.63(7)	N10—N8—C3	111.43(19)
O5i—Ti1—N1	80.63(7)	C17—C9—C6	120.9(2)
O5—Ti1—O2	91.51(8)	N8—N10—C4	104.43(17)
O5—Ti1—O2 ⁱ	162.68(6)	C13—C11—C4	120.3(2)
O5i—Ti1—O2	162.68(6)	C14—C11—C4	119.0(2)
O5i—Ti1—O2 ⁱ	91.51(8)	C14—C11—C13	120.8(2)
O5i—Ti1—O5	92.05(13)	C20—C12—C7	121.3(2)
C3—N1—Ti1 ⁱ	126.66(13)	C11—C13—O5 ⁱ	120.4(2)
C4—N1—Ti1 ⁱ	128.54(13)	C15—C13—O5 ⁱ	120.2(2)
C4—N1—C3	104.80(16)	C15—C13—C11	119.3(2)
C7—O2—Ti1 ⁱ	142.20(14)	C16—C14—C11	118.6(3)
C6—C3—N1	127.25(18)	C19—C15—C13	120.3(3)
N8—C3—N1	107.51(19)	C19—C16—C14	121.1(3)
N8—C3—C6	125.2(2)	C20—C17—C9	121.7 (2)
N10—C4—N1	111.79(18)	C16—C19—C15	120.0(3)
C11—C4—N1	124.16(18)	C17—C20—C12	119.8(2)

^aSymmetry transformation used to generate equivalent atoms: (i) $-x, -y, -z + 1$.

\AA). The shorter $\text{Ti}—\text{O}$ bond lengths in comparison to the $\text{Ti}—\text{N}$ lengths is due to the hard acid character of $\text{Ti}(\text{IV})$.

Aqueous solution speciation studies reveal that, at concentrations between mid micromolar to low millimolar, $\text{Ti}(\text{deferasirox})_2$ remains very stable for a minimum of 4 days over the broad pH range of 4.3 (the pH if dissolved in water) to 7.4, as indicated by unchanging UV-vis and ^1H NMR spectra of the compound at these pH values (Figure 4). There is no evidence of ligand dissociation and subsequently of hydrolysis, even at 37 °C (Figure S1 in the Supporting Information). Any changes in the spectra at pH 4.3 and 7.4 are due to deprotonation of each of the benzoic acids of the two coordinated deferasirox ligands. The pH titration curve for $\text{Ti}(\text{deferasirox})_2$ (Figure S2 in the Supporting Information) is indicative of a weak diprotic acid with 1 equiv of base needed to get each of the inflection points. Due to the symmetrical nature of the compound, the pK_a values of the benzoic acids are similar ($pK_{a1}=5.7 \pm 0.2$ and $pK_{a2}=5.9 \pm 0.3$). The potentiometric study provides insight into the speciation of $\text{Ti}(\text{IV})$ deferasirox at micromolar concentrations, 1/2 metal/ligand ratio in the pH 4–8 range (Figure 5). At pH 4.0 and 50 μM concentration, the neutral $\text{Ti}(\text{deferasirox})_2$ constitutes 98% of the $\text{Ti}(\text{IV})$ species. At pH 5.8, the speciation consists of 28% $[\text{Ti}(\text{deferasirox})_2]^-$, 39% $[\text{Ti}(\text{deferasirox})_2]^{2-}$, and 34% $[\text{Ti}(\text{deferasirox})_2]^{2-}$. At pH 7.4, the speciation consists of 97% $[\text{Ti}(\text{deferasirox})_2]^{2-}$. This speciation model is supported by UV-vis spectroscopy and mass spectrometry. At pH 4.3 the UV-vis spectrum of $\text{Ti}(\text{deferasirox})_2$ shows a ligand to metal charge transfer (LMCT) band at 370 nm with an extinction coefficient of 11100 $\text{M}^{-1} \text{cm}^{-1}$. At pH 7.4, the LMCT band is slightly blue shifted to 365 nm due to the double deprotonation yielding $[\text{Ti}(\text{deferasirox})_2]^{2-}$. The extinction coefficient for the LMCT band is very similar ($11300 \text{ M}^{-1} \text{cm}^{-1}$). Mass spectrometry data suggest that the dominant species present in the pH 4–8 range has a metal/ligand ratio of 1/2 (Figure 4). A similar aqueous speciation behavior is proposed for $\text{Ti}(\text{BHPT})_2$ on the basis of comparable spectral data (Figure S3 in the Supporting Information). Full deprotonation of the single proton at the triazole rings is expected to occur at pH values greater than 7.4, generating the dianionic species $[\text{Ti}(\text{BHPT})_2]^{2-}$. Due to the very poor solubility of this compound in water, the pK_a value of the triazole ring proton could not be determined.

The reduction potentials of $\text{Ti}(\text{deferasirox})_2$ at pH 4.3 ($E^\circ = -0.839 \text{ V}$ vs NHE, $\Delta E = 59.3 \text{ mV}$) and pH 7.4 ($E^\circ = -0.905 \text{ V}$ vs NHE, $\Delta E = 98.9 \text{ mV}$) measured by cyclic voltammetry suggest that $\text{Ti}(\text{IV})$ will have a stable oxidation state because the values are too negative and are outside the biological window, which in the intracellular environment covers the range between -0.24 and -0.18 V .⁴⁷ ΔE values for the $\text{Ti}(\text{IV})/\text{Ti}(\text{III})$ reduction indicate reversibility at pH 4.3 and semi-reversibility at pH 7.4. These experiments could not be performed for $\text{Ti}(\text{BHPT})_2$ due to its poor water solubility but would be expected to yield comparable results. These data, in total, reveal that deferasirox and BHPT coordinative saturation highly stabilizes $\text{Ti}(\text{IV})$ against dissociation, precipitation, and changes in oxidation much like the case for STF.^{29,48,49} This stabilization effect is even superior to another cTfm ligand, N,N' -bis(*o*-hydroxybenzyl)ethylenediamine- N,N' -diacetic acid (HBED), used in previous studies by Tinoco et al.,^{49,50} which at concentrations between low micromolar to low millimolar serves as a tetraanionic hexadentate ligand at very acidic pH values but undergoes partial intramolecular dissociation due to metal hydrolysis in the pH 5.0–7.4 range. The $\text{Ti}(\text{IV})$

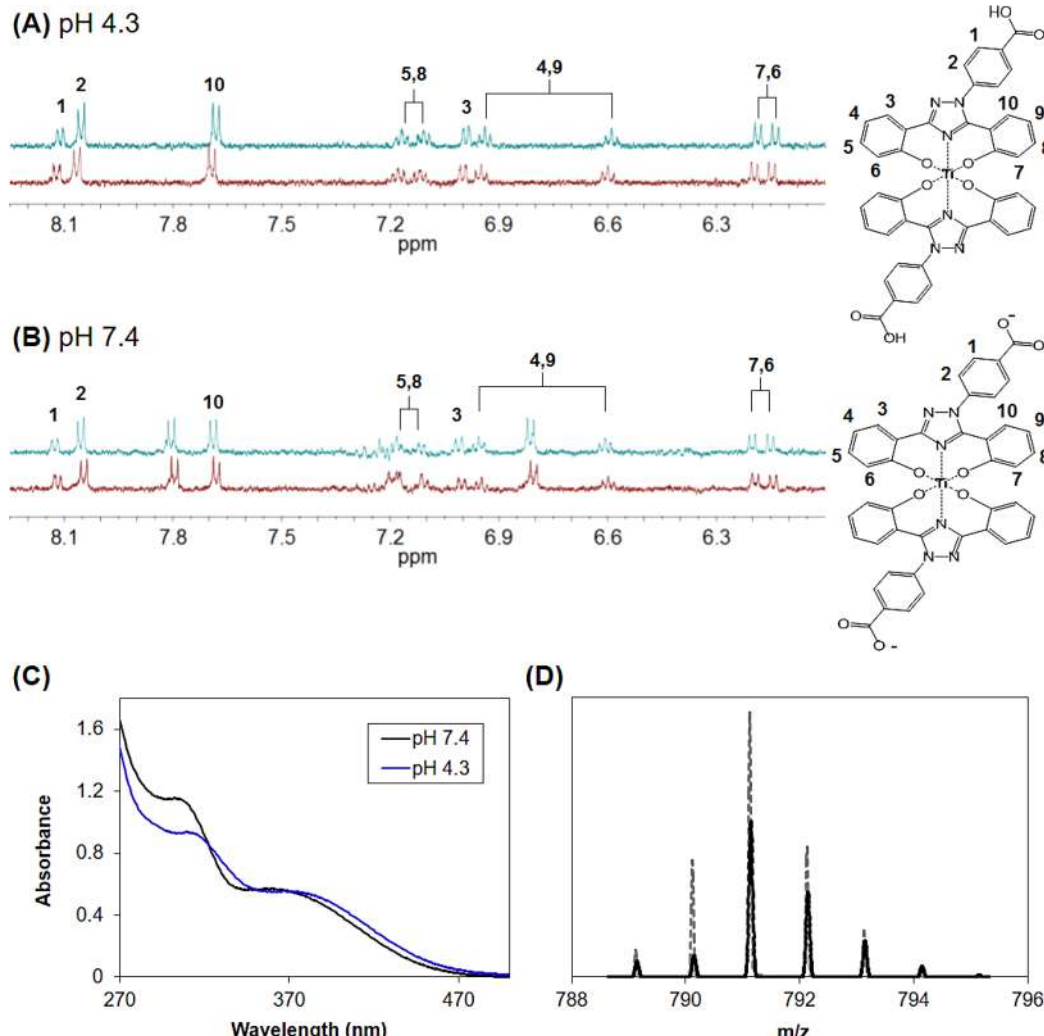


Figure 4. ^1H NMR spectrum of 50 μM $\text{Ti}(\text{deferasirox})_2$ (conditions: 500 MHz, 1/1 $\text{DMSO-d}_6/\text{D}_2\text{O}$): (A) pD 3.9, pH 4.3 (DCl); (B) pD 7.0, pH 7.4 (NaOD). The unchanging ^1H NMR of the compound at pH 4.3 and 7.4 suggests that there are no structural changes over a period of 4 days (0 h (red) to 96 h (blue)). Nevertheless, the chemical shift to upfield at pH 7.4 suggests a change in shielding induced by the deprotonation of the benzoic acid groups in concordance with the changes registered in (C) the UV-vis absorbance spectra of 50 μM $\text{Ti}(\text{deferasirox})_2$ at pH 4.3 and 7.4. (D) Positive ion mass spectrum of $\text{Ti}(\text{deferasirox})_2$ ($[\text{Ti}(\text{C}_{21}\text{H}_{14}\text{N}_3\text{O}_4)] + \text{H}^+$, m/z 791.573) detected in MALDI TOF/TOF. The experimental data (solid line) overlays the theoretical isotope distribution (dotted line).

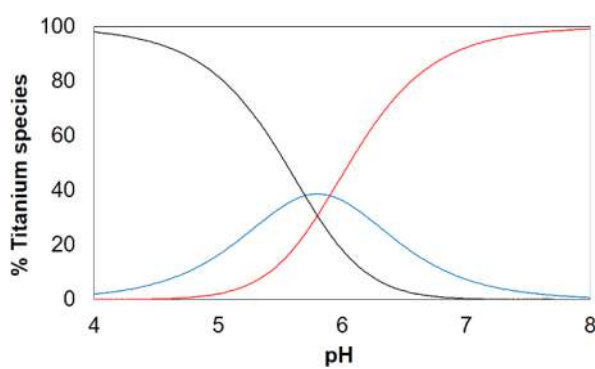


Figure 5. $\text{Ti}(\text{IV})$ deferasirox aqueous speciation from pH 4 to 8 using 50 μM $\text{Ti}(\text{IV})/100 \mu\text{M}$ deferasirox: (black line) $[\text{Ti}(\text{deferasirox})_2]^{0+}$; (blue line) $[\text{Ti}(\text{deferasirox})_2]^-$; (red line) $[\text{Ti}(\text{deferasirox})_2]^{2-}$.

deferasirox and BHPT complexes are also more stable than Tshuva et al.'s recently produced $\text{Ti}(\text{IV})$ complexes of N,N' -phenolate-substituted HBED derivative ligands, which after a few days in solution begin to exhibit hydrolytic behavior.⁵¹

$\text{Ti}(\text{IV})$ complexes of the siderophores enterobactin⁵² and desferrioxamine B,⁵³ iron chelators used by bacteria to scavenge iron, exhibit very high formation constants but have not been reported to display antiproliferative properties presumably because the $\text{Ti}(\text{IV})$ is too tightly held. Deferasirox and BHPT highly stabilize $\text{Ti}(\text{IV})$ in aqueous solution under physiologically relevant conditions for an indefinite period of time but can be induced to release the metal. This high stability and control of metal release bodes well for the application of these compounds as anticancer drugs.

Cell Viability Assays Revealing Different Cellular Responses to the $\text{Ti}(\text{IV})$ Complexes of Deferasirox and BHPT versus the Metal-Free Ligands. The human lung cell lines A549 (cancer) and MRC5 (normal) are model cell lines for examining the cytotoxic behavior of $\text{Ti}(\text{IV})$ complexes because they have been shown to respond to the identity of the ligands bound to the metal.^{35,50} A previous study of ours revealed that extremely labile $\text{Ti}(\text{IV})$ complexes such as titanocene dichloride are unable to induce cell death even at high micromolar concentrations.⁵⁰ Also, extremely inert $\text{Ti}(\text{IV})$

complexes are unable to kill the cells.⁵⁰ In a subsequent study, we discovered that the inertness of the Ti(IV) complex does not limit the cytotoxicity of the complex as long as its lability can be induced under physiological conditions and the Ti(IV) can be released. This induced lability is part of the application of cTfm ligands in our drug design strategy.³⁵ Using the A549 and MRC5 cells, we examined the effect that the high stabilization provided by deferasirox and BHPT to Ti(IV) would have on the potential cytotoxicity of the Ti(IV) complexes of these cTfm ligands. $[\text{Ti}(\text{deferasirox})_2]^{2-}$ showed a highly dose dependent antiproliferative effect against both cell lines, whereas $[\text{Ti}(\text{BHPT})_2]^{2-}$ demonstrated this behavior but only against the A549 cells (Table 2 and Figure 5). The

Table 2. IC₅₀ Values for Cell Viabilities of A549 and MRC5 Cells Treated with Metal-Free and Ti(IV)-Bound Complexes of cTfm Ligands

	IC ₅₀ , μM	
	A549	MRC5
$[\text{TiOHBED}]^-$ ^a	24.1 ± 1.2	42 ± 4
$[\text{Ti}(\text{deferasirox})_2]^{2-}$	20 ± 1	25 ± 1
$[\text{Ti}(\text{BHPT})_2]^{2-}$	6.6 ± 1.7	$\sim 2.3^b$
deferasirox	12.1 ± 1^c	^d
BHPT	^d	>100

^aData taken from ref 31. ^bRelative IC₅₀. ^cThis value was determined by fitting only the antiproliferative behavior of the data. ^dA proliferative behavior was observed.

compound $[\text{Ti}(\text{BHPT})_2]^{2-}$ showed a small antiproliferative effect against MRC5 cells. The complexes exhibited their antiproliferative effect even after a 30 day incubation in cell media at different temperatures (4, 25, 37 °C), a result that further emphasizes their high aqueous solution stability especially in comparison with $[\text{TiOHBED}]^-$, which loses all

cytotoxicity in the 30 day incubation at 37 °C (Figure S4 in the Supporting Information). $[\text{Ti}(\text{deferasirox})_2]^{2-}$ and $[\text{Ti}(\text{BHPT})_2]^{2-}$ demonstrate greater activity than $[\text{TiOHBED}]^-$ against the A549 cells. Interestingly, the metal-free ligands exhibited (in some cases) proliferative activity, although the behavior was more pronounced for deferasirox than for BHPT especially in MRC5 cells (Figure 6). To confirm that this proliferative activity was actually being detected and was not the product of an absorbance spike in the colorimetric viability assay, pictures of the MRC5 cells treated with the Ti(IV) compounds and the metal-free ligands at relevant concentrations were taken (Figure S5 in the Supporting Information). For deferasirox, this proliferative behavior was only a subset of the A549 data. In the majority of the data, deferasirox does indeed show a dose-dependent antiproliferative effect against A549, which compares favorably with the generally high cytotoxic behavior reported for this ligand. Deferasirox is considered to be a promising chemotherapeutic because of its ability to trigger cell death via different pathways and its ease of oral administration. In vitro studies demonstrate that deferasirox induces DNA fragmentation and the inhibition of DNA synthesis in both cancer and normal liver cell lines.³⁹ Deferasirox has also shown dose-dependent caspase-related apoptotic activity against leukemia cell lines.⁵⁴ Methoxy- and imidazole-substituted derivatives of deferasirox have shown antiproliferative activity related to iron depletion in lysosomes of treated cancerous liver and prostate cell lines in the range of submicromolar to micromolar concentrations.⁵⁵ Some of this promise is hindered by the nephrotoxicity frequently present in young and elderly patients after many years of therapy.⁵⁶ The finding of a proliferative effect in both cancer and normal cells, for undetermined reasons, further limits the application of deferasirox (or even BHPT) alone as an anticancer agent. This is a limitation not observed for the Ti(IV) complexes of the ligands, possibly because the proliferative effect of the ligands

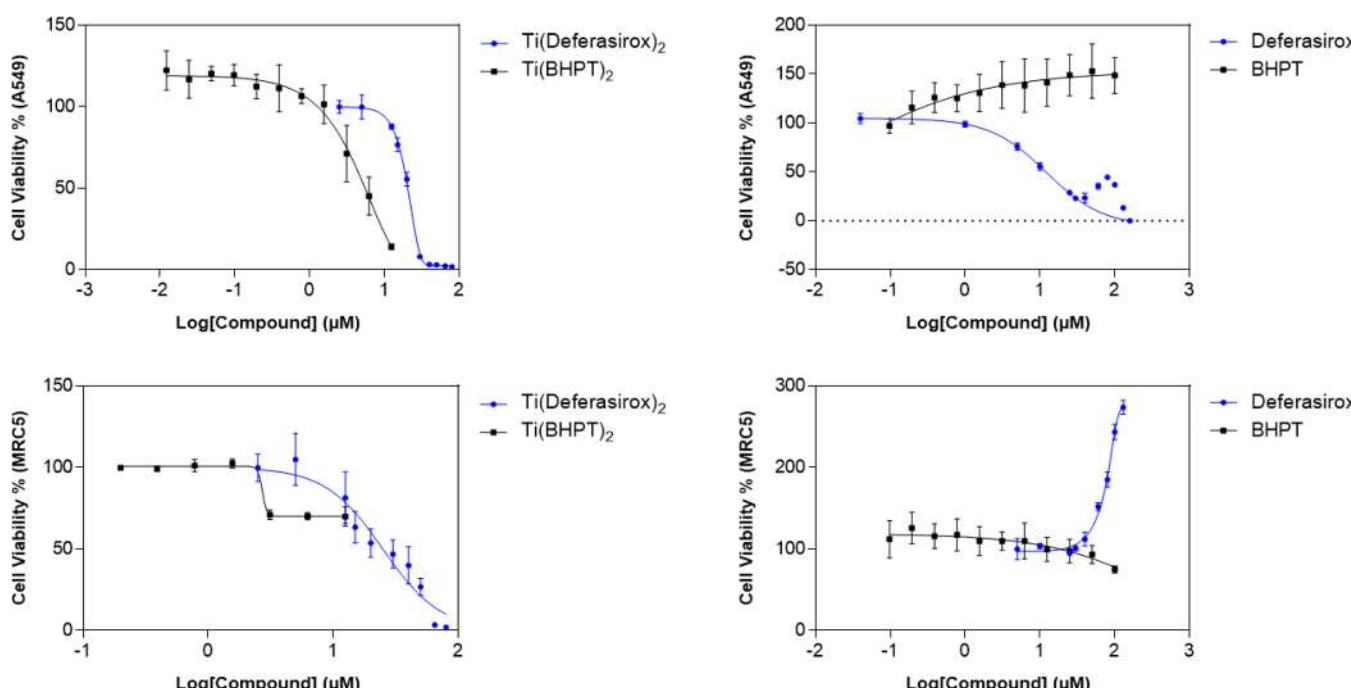


Figure 6. Dose–response curves for $[\text{Ti}(\text{deferasirox})_2]^{2-}$, $[\text{Ti}(\text{BHPT})_2]^{2-}$, and metal-free ligands against A549 lung cancer and MRC5 normal lung cell viability.

requires that they remain a free molecule and is independent of their metal binding capacity. Our characterization of the Fe(III) binding capacity of the Ti(IV) complexes and the metal-free ligands in later paragraphs will help to support this rationale.

The main limitation of $[\text{Ti}(\text{BHPT})_2]^{2-}$ is its limited solubility. In an attempt to improve the aqueous solubility of the complex, the use of a commonly used detergent in cell work, Triton X-100, was implemented at low concentration aimed to achieve not only an increase of solubility but also permeabilization of the membrane to allow greater cellular uptake of the compound. Standards prepared at the concentration range of 2–30 μM were incubated with A549 and MRC5 cells, which after 24 h did not survive due to extensive lysis. In addition, the standards were used to plot a calibration curve (concentration vs absorbance at 415 nm, Figure S6 in the Supporting Information) to determine the maximum solubility of $[\text{Ti}(\text{BHPT})_2]^{2-}$ dissolved in 0.1% Triton X-100 (PBS, 1% DMF, pH 7.4). By measuring the absorbance of the supernatant at 415 nm, it was determined that the maximum concentration achieved under these solution conditions is $31.5 \pm 0.9 \mu\text{M}$, which constitutes a 2-fold improvement in solubility, but with no improvement of compound activity against cancer cells. The difficulties represented by the poor aqueous solubility of $[\text{Ti}(\text{BHPT})_2]$ imply that its IC_{50} value against MRC5 cannot be accurately determined, perhaps because higher concentrations are required to achieve a lower percentage of cell viability.

Serum Proteins and Other Relevant Biomolecules Playing No Role in the Transport and Cytotoxicity of $[\text{Ti}(\text{deferasirox})_2]^{2-}$. Previous studies have demonstrated a direct correlation between the identity of the ligand and the cytotoxicity of Ti(IV) complexes.^{29,35,50,51,57} The ligands regulate not only the stability of Ti(IV) in solution but also its transport into cells, particularly if the complex can interact with serum biomolecules. Multiple *in vitro* studies have shown that, for anticancer platinum complexes, metal interaction with the protein components in serum-containing medium lowers the cytotoxicity of the complexes.⁵⁸ Ott, Tshuva, and Tacke revealed intriguing differences in the cellular Ti(IV) accumulation from a member of their respective family of Ti(IV) complexes.⁵⁹ Cells grown in serum-containing media resulted in significantly lower cellular accumulation of Ti(IV) from the titanocenes but much higher accumulation from the Ti(IV) salan complexes relative to the serum-free media. It is hypothesized that different serum protein interactions with the complexes is the source of this difference in cellular accumulation. Ott, Tshuva, and Tacke reported differences in serum albumin (SA) binding by the Ti(IV) salan complex and the titanocene complex, with the titanocene complex having much higher affinity to the protein.⁵⁹ Normally this would be seen as an advantage for improved uptake of the titanocenes, considering cancer cells uptake a higher quantity of albumin for metabolic purposes.⁶⁰ In our recent review on the molecular mechanisms that regulate Ti(IV) transport and its cytotoxicity, we speculate that SA binding deters the cellular accumulation of the titanocenes and lowers its cytotoxicity.⁸ We also suggest that the synergistic interaction of citrate and STf in binding Ti(IV) from labile sources in a very stable and hydrolysis-free form and in transporting the metal ion to cells may work to transform the Ti(IV) into a noncytotoxic species and thus attenuate titanocene cytotoxicity.

The higher cellular Ti(IV) accumulation exhibited by the Ti(IV) salan complexes in serum-containing media might also

be explained by our recent finding of the synergism between citrate and serum transferrin in binding and transporting Ti(IV) (from labile sources) into cells.²⁹ The Ti(IV) salan complexes in general are prone to hydrolysis in water on the time scale of minutes to hours⁶¹ but in the presence of serum levels of citrate ($\sim 100 \mu\text{M}$) are likely to undergo even faster dissociation due to competitive binding by citrate. This, in turn, would facilitate delivery of Ti(IV) to STf and could result in elevated Ti(IV) accumulation. Our work with the cTfm ligand HBED demonstrated that high concentrations of citrate (1 mM) can induce the dissociation of the highly stable Ti(IV) complex of the ligand ($[\text{TiOHBED}]^-$).²⁹ Citrate facilitates significant Ti(IV) loading of serum levels of STf (~ 30 – $60 \mu\text{M}$).^{29,62} $[\text{TiOHBED}]^-$, like Tshuva's Ti(IV) salan compound, does not bind to SA.⁵⁰ A549 and MRC5 cell viability studies revealed that the net effect of the citrate- and STf-induced dissociation of $[\text{TiOHBED}]^-$ was a decrease in the cytotoxicity of the complex.^{29,50} The product $\text{Ti}_2\text{-STf-(CO}_3)_2\text{(citrate)}_2$ does not demonstrate any cytotoxicity in these cell lines even at 100 μM (Figure 1). No correlation between possible changes in Ti(IV) salan cytotoxicity and the elevated Ti(IV) cellular accumulation due to serum were actually established.⁵⁹

In light of the effect that SA, STf, and citrate have on the serum speciation of Ti(IV) complexes and Ti(IV) accumulation in cells, the interaction of these biomolecules with micromolar levels of $[\text{Ti}(\text{deferasirox})_2]^{2-}$ was examined at pH 7.4. The next set of solution-based experiments could not be performed with $[\text{Ti}(\text{BHPT})_2]^{2-}$ due to its poor water solubility and subsequently low detection at the concentrations that could be achieved. An equilibrium dialysis study performed by reacting different concentrations of $[\text{Ti}(\text{deferasirox})_2]^{2-}$ (10–70 μM) with SA ($\sim 300 \mu\text{M}$) showed that the complex did not bind to the protein. Following the reaction, there was no evidence in the UV-vis spectrum of the dialyzed protein of the LMCT absorbance at 365 nm, characteristic of the metal complex. There was also no measurable Ti(IV) content in the protein fraction. $[\text{Ti}(\text{deferasirox})_2]^{2-}$ also remained fully intact in the presence of physiological amounts of STf and citrate over the course of 3 days. The UV-vis spectrum of the complex remains unchanged, indicating no dissociation of the complex. In addition, after an aliquot of the protein was dialyzed daily, no growth in a LMCT absorbance at 321 nm due to the formation of $\text{Ti}_2\text{-STf-(CO}_3)_2\text{(citrate)}_2$ complex was observed.^{29,63} $[\text{Ti}(\text{deferasirox})_2]^{2-}$ did not dissociate even in the presence of 5 mM citrate concentration over the same time frame (Figure S7 in the Supporting Information).

These studies together suggest that SA, STf, and citrate will not contribute to the Ti(IV) accumulation in cells by $[\text{Ti}(\text{deferasirox})_2]^{2-}$ or to any cytotoxicity it exhibits. An additional biomolecule from the extracellular environment to consider in this analysis, which is not typically evaluated when studying Ti(IV) compounds with anticancer properties, is Fe(III)-bound STf (Fe₂-STf). Considering that it is thermodynamically feasible for Fe(III) to displace Ti(IV) from deferasirox coordination due to its very high affinity for Fe(III) at pH 7.4 (forming the $[\text{Fe}(\text{deferasirox})_2]^{3-}$ species³⁷) and that Fe₂-STf is the main Fe(III) species in blood, we evaluated $[\text{Ti}(\text{deferasirox})_2]^{2-}$ stability in the presence of physiological levels of Fe₂-STf. At pH 7.4 Fe₂-STf was incubated with $[\text{Ti}(\text{deferasirox})_2]^{2-}$ and the metal-free ligand for 72 h. At 24 h time intervals, an aliquot of the reaction was dialyzed extensively. The Fe(III) content in STf was determined by monitoring the Fe₂-STf LMCT at λ 465 nm ($\epsilon = 5200 \text{ M}^{-1}$

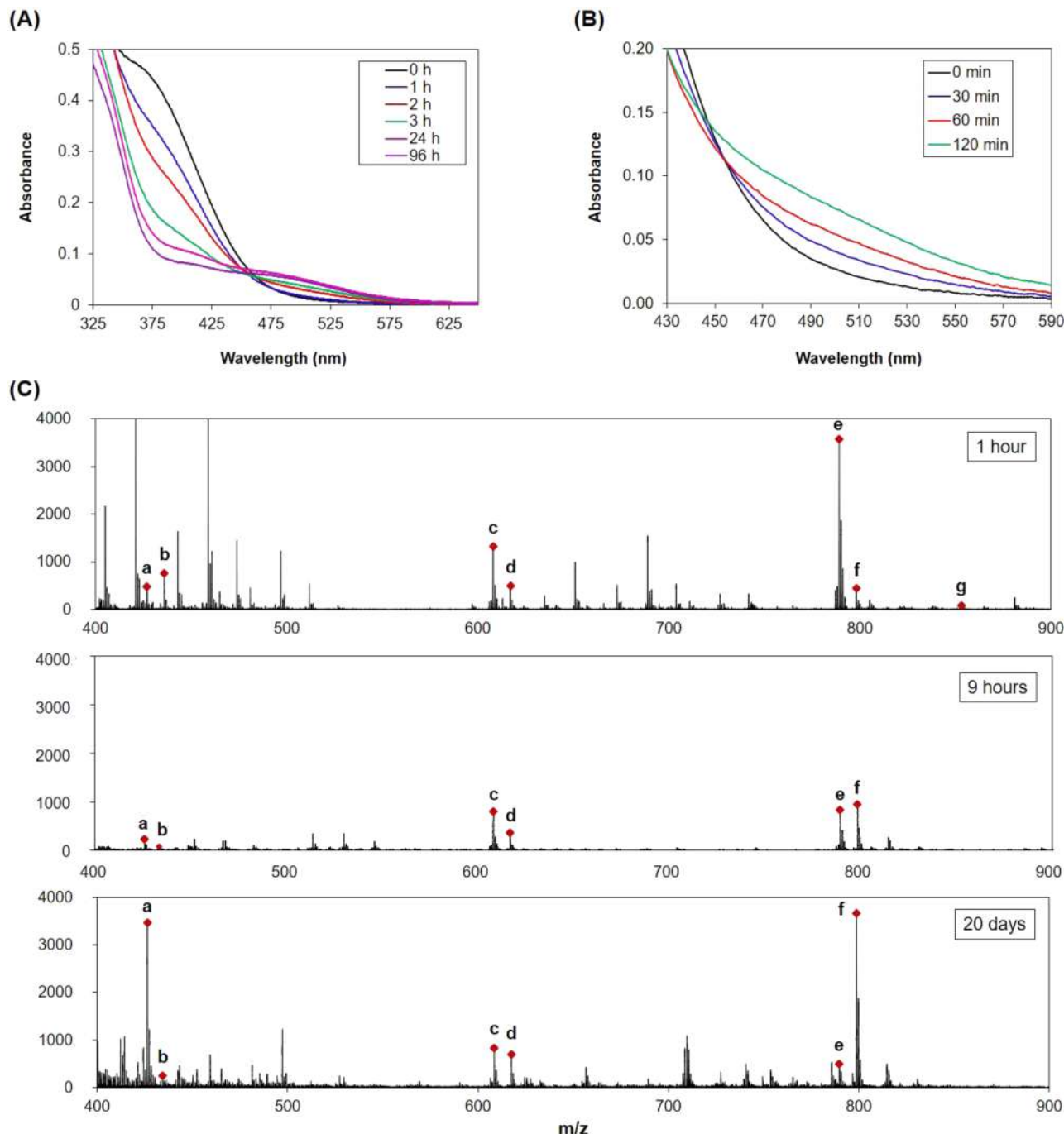
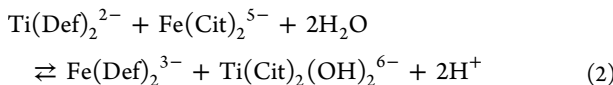


Figure 7. (A) UV-vis absorbance spectra of monitored reaction between $50 \mu\text{M} [\text{Ti(deferasirox)}_2]^{2-}$ and $50 \mu\text{M} [\text{Fe(citrate)}_2]^{5-}$ at pH 7.4 (Tris 20 mM, NaCl 1 M). (B) Absorbance spectrum of monitored reaction between $50 \mu\text{M} [\text{Ti(deferasirox)}_2]^{2-}$ and $50 \mu\text{M} [\text{Fe(citrate)}_2]^{5-}$ at pH 7.4 in the presence of 5 mM of citrate (Tris 20 mM, NaCl 1 M). (C) Negative mode mass spectrum of the reaction between $50 \mu\text{M} [\text{Fe(citrate)}_2]^{5-}$ and $50 \mu\text{M} [\text{Ti(deferasirox)}_2]^{2-}$ at pH 7.4. The reaction was monitored at 1 h, 9 h, and 20 days. Data suggest a multistep transmetalation process involving the following species: (a) $[\text{Ti(citrate)}_2]^{4-}$, (b) $[\text{Fe(citrate)}_2]^{5-}$, (c) $[\text{Ti(deferasirox)}(\text{citrate})]^{3-}$, (d) $[\text{Fe(deferasirox)}(\text{citrate})]^{4-}$, (e) $[\text{Ti(deferasirox)}_2]^{2-}$, (f) $[\text{Fe(deferasirox)}_2]^{3-}$, and (g) $[\text{Ti(deferasirox)}\text{Fe(citrate)}_2]^{4-}$.

cm^{-1}) using UV-vis spectroscopy. However, no loss in the signal for the LMCT band was observed in either the reactions with the complex or surprisingly with the free ligand, indicating that the protein remained Fe(III)-saturated at all three time points. This result highlights the high stability that $[\text{Ti(deferasirox)}_2]^{2-}$ is expected to exhibit during blood transport and suggests that no disruption of the normal iron homeostasis would occur due to the lack of interaction between $\text{Fe}_2\text{-STf}$ and $[\text{Ti(deferasirox)}_2]^{2-}$ and free deferasirox (Figure 2).

Deferasirox Transmetalation from Ti(IV) to Fe(III) Induced by a Labile Fe(III) Intracellular Source. Within the cytosol (pH 7.4) a labile Fe(III) pool exists that has the capacity to interact with $[\text{Ti(deferasirox)}_2]^{2-}$ and destabilize it. A kinetic metal binding competition experiment was conducted to examine the time frame for a Ti(IV) to Fe(III) deferasirox transmetalation using Fe(III) citrate ($[\text{Fe(citrate)}_2]^{5-}$), a labile low-molecular-weight nontransferrin bound iron (NTBI) species⁶⁴ that can exist in cells. An equimolar ($50 \mu\text{M}$) reaction

was performed between $[\text{Ti}(\text{deferasirox})_2]^{2-}$ and $[\text{Fe}(\text{citrate})_2]^{5-}$ and monitored over time by UV-vis and mass spectrometry (eq 2).



A color change occurs rapidly after mixing the two solutions; however, the UV-vis spectrum does not show distinct isosbestic points to distinguish among reactants, intermediates, and products. During the 24 h that the reaction was monitored by UV-vis (325–600 nm wavelength), the disappearance of the LMCT absorbance of $[\text{Ti}(\text{deferasirox})_2]^{2-}$ was detected followed by the subsequent formation of the LMCT absorbance of $[\text{Fe}(\text{deferasirox})_2]^{-}$ ($\lambda = 420 \text{ nm}$, $\epsilon = 5720 \text{ M}^{-1} \text{ cm}^{-1}$; $\lambda = 477 \text{ nm}$, $\epsilon = 4050 \text{ M}^{-1} \text{ cm}^{-1}$)³⁷ (Figure 7a). To gain insight into the overall transmetalation mechanism, a high concentration of citrate (5 mM) was included to slow down the reaction and to better observe the initial part of the transmetalation. As already discussed, 5 mM citrate alone does not remove Ti(IV) from deferasirox. That Ti(IV) release does occur in the presence of $[\text{Fe}(\text{citrate})_2]^{5-}$ suggests that the transmetalation is triggered by labile Fe(III). A new UV-vis absorbance for an intermediate species appears at the beginning of the reaction displaying an isosbestic point ($\lambda = 454 \text{ nm}$) (Figure 7b). After 60 min this absorbance then transitions to the spectral features characteristic of the reaction in the absence of high citrate concentration (Figure 7a). A plot of the observed rate constant for the formation of this species (at the initial time points) versus $[\text{Fe}(\text{citrate})_2]^{5-}$ concentration demonstrates a hyperbolic growth dependence indicative of an intermediate required for this species to form (Figure 8).

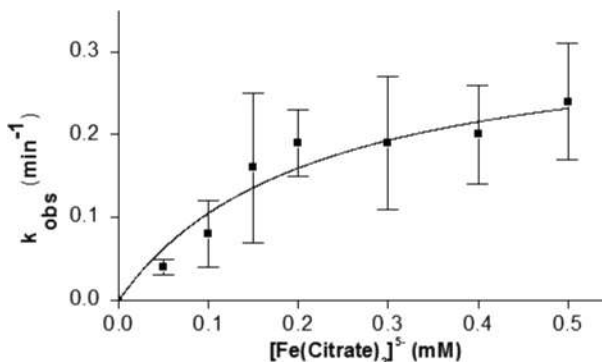
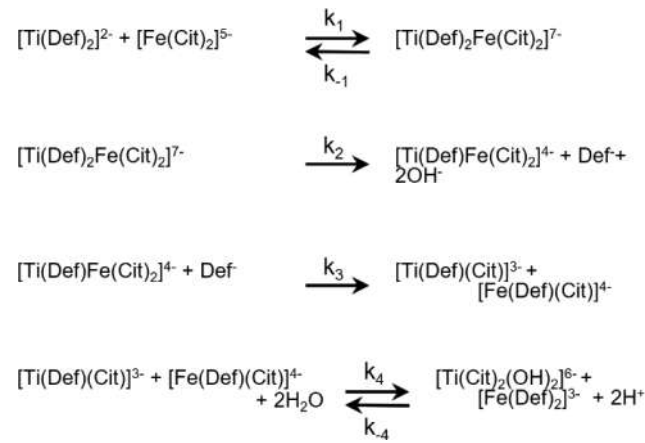


Figure 8. Plot of the dependence of the observed rate constant for $[\text{Ti}(\text{deferasirox})\text{Fe}(\text{citrate})_2]^{4-}$ formation on the concentration of $[\text{Fe}(\text{citrate})_2]^{5-}$ from the reaction of $[\text{Ti}(\text{deferasirox})_2]^{2-}$ and $[\text{Fe}(\text{citrate})_2]^{5-}$ in the presence of a high citrate background (5 mM). The data were fit to eq 3 using nonlinear iterative regression.

Mass spectrometric analysis (Figure 7c and Figure S8 in the Supporting Information) suggests that the transmetalation process is multistep involving the formation of several intermediates (Scheme 1). MS data were collected for the equimolar reaction of $[\text{Ti}(\text{deferasirox})_2]^{2-}$ and $[\text{Fe}(\text{citrate})_2]^{5-}$ but not at high citrate concentration, to prevent interference from the high salt content and to maintain physiologically relevant conditions. The data suggest that $[\text{Ti}(\text{deferasirox})\text{Fe}(\text{citrate})_2]^{4-}$ is a likely candidate for the species producing the new absorbance observed in the high-citrate UV-vis experiments (Figure 7b). The m/z signal for this species (Figure S8)

Scheme 1. Proposed Mechanism for Deferasirox Transmetalation of Ti(IV) for Fe(III) without Excess Citrate Background



was of a very low intensity. It is proposed that, for this species to form, the bimetallic complex $[\text{Ti}(\text{deferasirox})_2\text{Fe}(\text{citrate})_2]^{7-}$ must first be generated, which then leads to a dissociation of one deferasirox ligand (Figure S8).

A rate equation (eq 3) was derived for the formation of the $[\text{Ti}(\text{deferasirox})\text{Fe}(\text{citrate})_2]^{4-}$ species, which properly fits the high citrate data (Figure 8), where k_2 is $0.33 \pm 0.08 \text{ min}^{-1}$ and K is $0.21 \pm 0.11 \text{ M}$ (Supporting Information).

$$\begin{aligned} \frac{d\{[\text{Ti(Def)}_2\text{Fe(Cit)}_2]^{7-}\}}{dt} \\ = \frac{k_2[\text{Fe(Cit)}_2]^{5-}\{[\text{Ti(Def)}_2]^{2-}\}_{\text{init}}}{\frac{k^{-1} + k_2}{k_1} + [\text{Fe(Cit)}_2]^{5-}} \\ = \frac{k_2[\text{Fe(Cit)}_2]^{5-}\{[\text{Ti(Def)}_2]^{2-}\}_{\text{init}}}{K + [\text{Fe(Cit)}_2]^{5-}} \\ = k_{\text{obs}}\{[\text{Ti(Def)}_2]^{2-}\}_{\text{init}} \end{aligned} \quad (3)$$

The mass spectral data also reveal subsequent steps of the reaction performed in the absence of excess citrate that suggest an overall mechanism of transmetalation (Scheme 1), which supports the proposed eq 3. The products $[\text{Fe}(\text{deferasirox})_2]^{3-}$ and $[\text{Ti}(\text{citrate})_2]^{4-}$ are observed to form in small amounts during the first 1 h of the reaction and become the dominant species when the reaction reaches equilibrium (Figure 7b). At the concentration of Ti(IV) (50 μM) and citrate (100 μM) used for this experiment, an aqueous speciation model predicts that the species $[\text{Ti}(\text{citrate})_2(\text{OH})_2]^{6-}$ is virtually 100% dominant at pH 7.4 (Figure S9 in the Supporting Information).⁶⁵ We have previously synthesized the sodium salt of this species in the solid state.⁴⁸ By mass spectrometry the species in solution is detected as $[\text{Ti}(\text{citrate})_2]^{4-}$, likely due to instrumental protonation of the citrate and hydroxo ligands. The aqua ligands that form from the hydroxo groups are believed to be dissociated during the electrospray ionization process, as we have typically been unable to detect them in any metal complexes. A slightly modified reaction scheme is presented in Scheme S1 in the Supporting Information for the reaction in the presence of excess citrate because under these conditions $[\text{Ti}(\text{citrate})_3]^{8-}$ is 100% dominant (Figure S9).⁶⁵ An extensive characterization of the reaction scheme was not performed because it is outside the scope of the article's

focus. The data as a whole elucidate that $[\text{Ti}(\text{deferasirox})_2]^{2-}$ in the presence of a labile Fe(III) source can rapidly undergo intracellular transmetalation with Fe(III). The net effect is a lowering of Fe(III) bioavailability and possible transfer of Ti(IV) to an intracellular site (Figure 2).

Fe(III) Chelation and Late Apoptosis Induction Constituting Part of the Mechanism of Action of the $[\text{Ti}(\text{deferasirox})_2]^{2-}$ and $[\text{Ti}(\text{BHPT})_2]^{2-}$ Species. To evaluate the role of iron chelation in the cytotoxic mechanism of the $[\text{Ti}(\text{deferasirox})_2]^{2-}$ and $[\text{Ti}(\text{BHPT})_2]^{2-}$ species, an Fe(III) supplementation experiment was performed. A549 and MRC5 cells were pretreated with different concentrations of $[\text{Fe}(\text{citrate})_2]^{5-}$ (40, 100, and 150 μM) to determine whether addition of Fe(III) would help the cells to resist the effects of $[\text{Ti}(\text{deferasirox})_2]^{2-}$, $[\text{Ti}(\text{BHPT})_2]^{2-}$, and the metal-free ligands, presumably by preventing intracellular Fe(III) depletion.

For the A549 cells without treatment with the Ti(IV) compounds or ligands, Fe(III) supplementation increased the viability of the cells, which is expected because cancer cells have a higher requirement for Fe(III). In contrast, for MRC5 cells the higher two concentrations of supplemented Fe(III) decreased viability perhaps due to exceeding homeostatic levels of Fe(III) in these healthy cells. The elevated Fe(III) pool in these cells can be transformed to redox-active Fe(II) because of the reducing environment of cells, which can lead to excessive production of reactive oxygen species.⁶⁶ It should be noted that, for all experiments performed with MRC5 and treatment with 150 μM $[\text{Fe}(\text{citrate})_2]^{5-}$, a decrease in cell viability is always observed. Fe(III) supplementation decreases the cell proliferative property of metal-free deferasirox observed in MRC5 cells, notably at the higher two concentrations. This result indicates that the proliferative property of deferasirox is not associated with its Fe(III) binding capacity.

The Fe(III) supplementation significantly improves the viability of the A549 cells against $[\text{Ti}(\text{deferasirox})_2]^{2-}$ and deferasirox and of MRC5 against $[\text{Ti}(\text{deferasirox})_2]^{2-}$ (Figure 9). The improvement is marginal in the A549 and MRC5 cell viabilities against $[\text{Ti}(\text{BHPT})_2]^{2-}$ and BHPT (Figure S10 in the Supporting Information). An improvement in the viability of the cells against $[\text{TiOHBED}]^-$ was also observed following Fe(III) supplementation.³⁵ In these cell lines, the Fe(III) version of the deferasirox³⁷ and BHPT complexes ($[\text{Fe}(\text{deferasirox})_2]^{3-}$ and $[\text{Fe}(\text{BHPT})_2]^{6-}$ (proposed)) demonstrate little to no cytotoxic behavior at concentrations equal to or higher than those of their Ti(IV) counterparts because they are already Fe(III) bound. These results support the importance of Fe(III) chelation in the mechanism of action of Ti(IV) cTfm complexes. In addition to the intrinsic cytotoxicity of the Ti(IV) species, the capture of bioavailable Fe(III) in the intracellular space directly interferes with the homeostasis of this essential metal and would inhibit accessibility of the metal to cancerous cells. In this context, it is important to determine the change in the iron pool within the cells treated with $[\text{Ti}(\text{deferasirox})_2]$ and $[\text{Ti}(\text{BHPT})_2]$ by performing a combination of quantitative elemental analysis and electron paramagnetic resonance approaches.

Additional insight into the cytotoxic mechanism of $[\text{Ti}(\text{deferasirox})_2]^{2-}$, $[\text{Ti}(\text{BHPT})_2]^{2-}$, and the metal-free ligands was obtained by evaluating their ability to induce apoptosis, a regulated process of cell death. The Alexa Fluor 488 Annexin V/Dead Cell Apoptosis Kit was used for this purpose. A549 cells were treated with buffer alone (negative control),

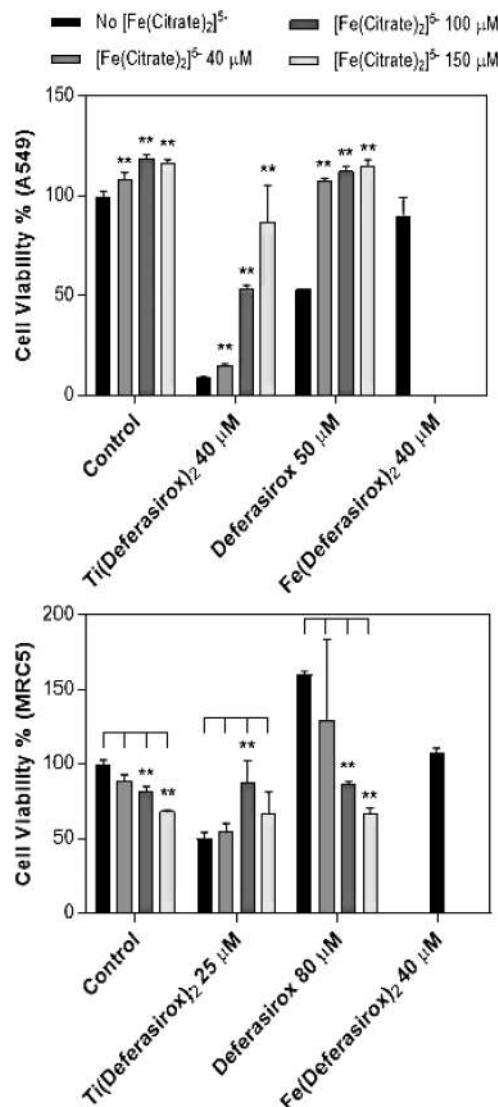


Figure 9. A549 and MRC5 cell viabilities against $[\text{Ti}(\text{deferasirox})_2]^{2-}$ and deferasirox measured in the presence (gray tones) and absence (black) of $[\text{Fe}(\text{citrate})_2]^{5-}$. The cells were also treated with $[\text{Fe}(\text{deferasirox})_2]^{3-}$ (** Student's *t* test, p value $\ll 0.01$, $n = 4$, mean \pm SD).

$[\text{Ti}(\text{deferasirox})_2]^{2-}$, $[\text{Ti}(\text{BHPT})_2]^{2-}$, and the metal-free ligands (Figure 10). The control cells demonstrate insignificant fluorescence because they are alive and nonapoptotic.

The cells treated with $[\text{Ti}(\text{deferasirox})_2]^{2-}$, $[\text{Ti}(\text{BHPT})_2]^{2-}$, and the ligands exhibit green fluorescence emission from the Alexa Fluor Alexa Fluor 488 Annexin V, due to the externalization of phosphatidyl serine on the cell membrane characteristic of the early apoptotic machinery activation. The propidium iodine red fluorescence in the nuclei shows chromatin condensation and activation of late apoptosis due to the disruption of the cell membrane.

These data indicate that the metal compounds and the ligands trigger early and late apoptosis. This apoptotic behavior appears to be a general property of the Ti(IV) cTfm complexes, as it is also observed with $[\text{TiOHBED}]^-$ (also HBED) (Figure 10) and Tshuva et al.'s Ti(IV) complexes of *N,N'*-phenolate-substituted HBED derivative ligands.⁵¹ The ability to induce apoptosis is a property that has been observed for metal-free

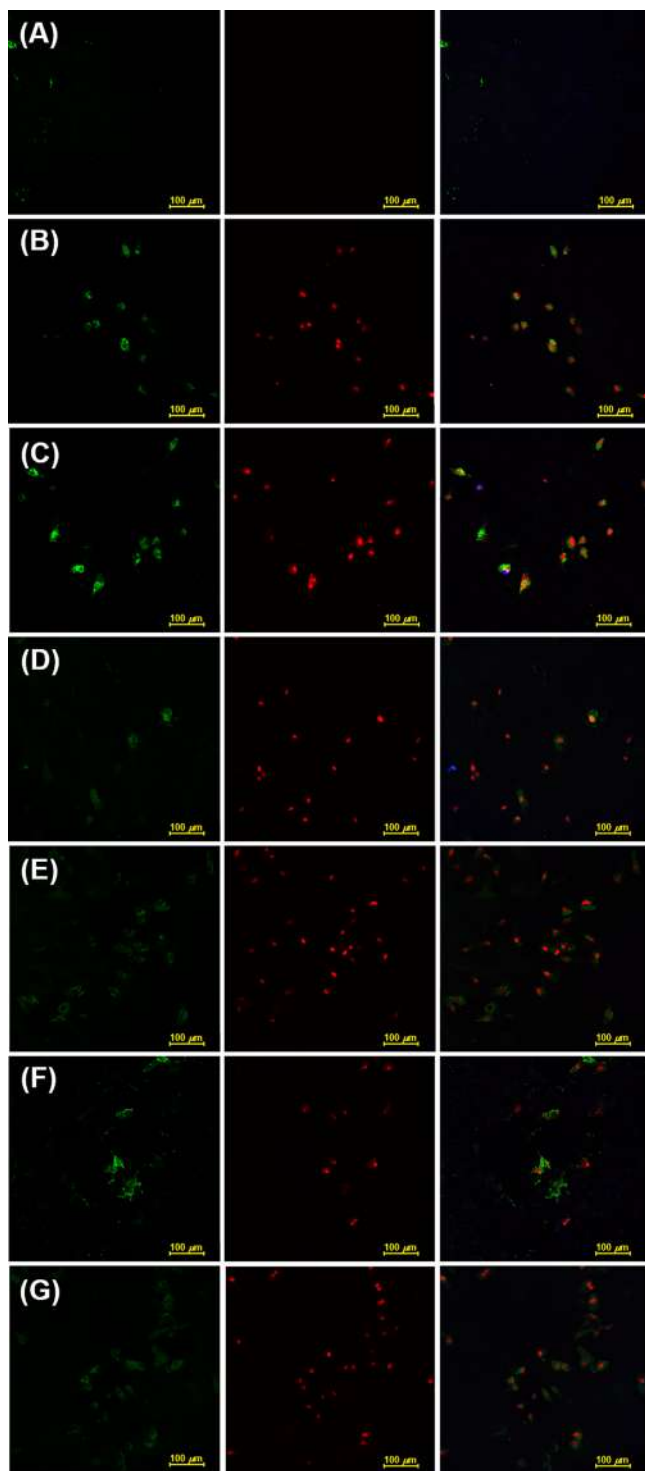


Figure 10. Apoptosis activation in A549 cells using Annexin V and propidium iodide after 24 h of incubation (images scaled to 100 μm): (A) untreated cells; (B) 50 μM $[\text{Ti}(\text{deferasirox})_2]^{2-}$; (C) 50 μM deferasirox; (D) 30 μM $[\text{Ti}(\text{BHPT})_2]^{2-}$; (E) 30 μM BHPT; (F) 50 μM $[\text{TiOHBED}]^-$; (G) 50 μM HBED. Cells undergoing early apoptosis exhibited a green fluorescence emission (left panel) from the Alexa Fluor Alexa Fluor 488 Annexin V. Cells undergoing late apoptosis exhibited red fluorescence due to propidium iodine (middle panel). The right panel demonstrates an overlay of the green and red fluorescence.

deferasirox³⁹ but not reported for BHPT, which may be attributed to its low cytotoxicity (Figure 6 and Table 2).

Whether the ability of $[\text{Ti}(\text{deferasirox})_2]^{2-}$, $[\text{Ti}(\text{BHPT})_2]^{2-}$, and $[\text{TiOHBED}]^-$ to trigger early and late apoptosis is associated with their Fe(III) chelation property requires further examination.

CONCLUSIONS

The selection of deferasirox as a cTfm ligand in our anticancer drug design strategy produces a potent cytotoxic Ti(IV) complex displaying some of the highest aqueous stabilities that have been observed. The complex remains stable in the presence of known serum biomolecular Ti(IV) binders and even escapes induced dissociation due to the synergistic binding of Ti(IV) by citrate and STf that has been shown to attenuate the cytotoxicity of other Ti(IV) complexes. Metal displacement kinetic studies show that, in approximating STf binding of Fe(III), deferasirox favors Fe(III) binding versus Ti(IV) and can rapidly bind Fe(III) via a transmetalation process and could eventually result in the delivery of Ti(IV) to intracellular target sites on a physiologically relevant time scale. This induced dissociation of Ti(IV) is only observed with a labile Fe(III) source, which implies that $[\text{Ti}(\text{deferasirox})_2]^{2-}$ should survive intact transport into cells and become activated intracellularly. Fe(III) supplementation studies performed alongside other Ti(IV) cTfm complexes generally support that the decrease of Fe bioavailability is part of their mechanism of action. The complexes also exhibit the capacity to trigger apoptosis. This activity may be correlated with their Fe(III) binding ability because the metal-free ligands also exhibit this behavior, but future investigations are required to establish this correlation. The data strongly point to the Ti(IV) cTfm complexes as superior antiproliferative agents in comparison to the metal-free ligands. These studies provide insight into the evolution of Ti(IV)-based anticancer drug design and into synthesizing derivatives of our parent compounds to improve the cancer cell selectivity of Ti(IV) cTfm compounds and the specificity of their activity.

ASSOCIATED CONTENT

Supporting Information

The Supporting Information is available free of charge on the ACS Publications website at DOI: [10.1021/acs.inorgchem.7b00542](https://doi.org/10.1021/acs.inorgchem.7b00542).

¹H nuclear magnetic resonance (NMR), mass spectra (MALDI TOF TOF), and experimental UV-vis spectra for $[\text{Ti}(\text{BHPT})_2]$, additional cell viability assay results, UV-vis stability evaluation for $[\text{Ti}(\text{deferasirox})_2]$, and mass spectra for the species involved in the transmetalation reaction ([PDF](#))

Accession Codes

CCDC 1441137 contains the supplementary crystallographic data for this paper. These data can be obtained free of charge via www.ccdc.cam.ac.uk/data_request/cif, or by emailing data_request@ccdc.cam.ac.uk, or by contacting The Cambridge Crystallographic Data Centre, 12 Union Road, Cambridge CB2 1EZ, UK; fax: +44 1223 336033.

AUTHOR INFORMATION

Corresponding Author

*E-mail for A.D.T.: atinoco9278@gmail.com.

ORCID iD

Arthur D. Tinoco: 0000-0003-2825-5235

Notes

The authors declare no competing financial interest.

ACKNOWLEDGMENTS

We thank the laboratory of Kai Griebenow (Manoj Saxena; Dr. Griselle Hernandez) at UPR RP for help with instruments and supplies. We also thank Mildred Rivera-Isaac at UPR RP for her help with mass spectrometry experiments, Javier Santos at Molecular Sciences Research Center (UPR) for his help with ICP-OES experiments, and Bismark Madera from the Molecular Characterization Center (UPR) with his help with confocal microscopy experiments. The confocal microscopy work was supported by the National Institute of General Medical Sciences (NIGMS) of the National Institutes of Health (NIH) under Award Number P20GM103642. S.A.L-R., A.D.T., and Y.D. are supported by the NIH SC1 (5SC1CA190504-02) provided by the NIGMS and NCI. A.D.T. is also supported by funding from the Puerto Rico Science, Technology, and Research Trust (Agreement No. 2013-000019), the University of Puerto Rico FIP Grant from the office of the DEGI, the University of Puerto Rico Score Stabilization Grant, and the Department of Chemistry at UPR RP.

REFERENCES

- (1) Keppler, B. K.; Friesen, C.; Moritz, H. G.; Vongerichten, H.; Vogel, E. Tumor-inhibiting bis(β -Diketonato) metal complexes. Budotitane, cis-diethoxybis(1-phenylbutane-1,3-dionato)titanium(IV). *Struct. Bonding* **1991**, *78*, 97–127.
- (2) Harding, M. M.; Mokdsi, G. Antitumour metallocenes: structure-activity studies and interactions with biomolecules. *Curr. Med. Chem.* **2000**, *7*, 1289–303.
- (3) Kostova, I. Titanium and vanadium complexes as anticancer agents. *Anti-Cancer Agents Med. Chem.* **2009**, *9*, 827–42.
- (4) Caruso, F.; Rossi, M. Antitumor Titanium Compounds. *Mini-Rev. Med. Chem.* **2004**, *4*, 49–60.
- (5) Schilling, T.; Keppler, K. B.; Heim, M. E.; Niebch, G.; Dietzfelbinger, H.; Rastetter, J.; Hanuske, A. R. Clinical phase I and pharmacokinetic trial of the new titanium complex budotitane. *Invest. New Drugs* **1995**, *13*, 327–332.
- (6) Toney, J. H.; Marks, T. J. Hydrolysis chemistry of the metallocene dichlorides M(eta.5-CSHS)2Cl₂, M = titanium, vanadium, or zirconium. Aqueous kinetics, equilibria, and mechanistic implications for a new class of antitumor agents. *J. Am. Chem. Soc.* **1985**, *107*, 947–953.
- (7) Meléndez, E. Titanium complexes in cancer treatment. *Crit. Rev. Oncol. Hematol.* **2002**, *42*, 309–315.
- (8) Loza-Rosas, S. A.; Saxena, M.; Delgado, Y.; Gaur, K.; Pandrala, M.; Tinoco, A. D. A ubiquitous metal, difficult to track: towards an understanding of the regulation of titanium(IV) in humans. *Metallomics* **2017**, *9*, 346–356.
- (9) Hernández, R.; Lamboy, J.; Gao, L. M.; Matta, J.; Román, F. R.; Meléndez, E. Structure–activity studies of Ti(IV) complexes: aqueous stability and cytotoxic properties in colon cancer HT-29 cells. *JBIC, J. Biol. Inorg. Chem.* **2008**, *13*, 685–692.
- (10) Hernández, R.; Méndez, J.; Lamboy, J.; Torres, M.; Román, F. R.; Meléndez, E. Titanium(IV) Complexes: Cytotoxicity and Cellular Uptake of Titanium(IV) Complexes on Caco-2 Cell Line. *Toxicol. In Vitro* **2010**, *24*, 178.
- (11) Allen, O. R.; Croll, L.; Gott, A. L.; Knox, R. J.; McGowan, P. C. Functionalized Cyclopentadienyl Titanium Organometallic Compounds as New Antitumor Drugs. *Organometallics* **2004**, *23*, 288–292.
- (12) Sweeney, N. J.; Mendoza, O.; Müller-Bunz, H.; Pampillón, C.; Rehmann, F.-J. K.; Strohfeldt, K.; Tacke, M. Novel benzyl substituted titanocene anti-cancer drugs. *J. Organomet. Chem.* **2005**, *690*, 4537–4544.
- (13) Potter, G. D.; Baird, M. C.; Cole, S. P. C. A new series of titanocene dichloride derivatives bearing cyclic alkylammonium groups: Assessment of their cytotoxic properties. *J. Organomet. Chem.* **2007**, *692*, 3508–3518.
- (14) Gao, L. M.; Vera, J. L.; Matta, J.; Meléndez, E. Synthesis and cytotoxicity studies of steroid-functionalized titanocenes as potential anticancer drugs: sex steroids as potential vectors for titanocenes. *JBIC, J. Biol. Inorg. Chem.* **2010**, *15*, 851–859.
- (15) Allen, O. R.; Gott, A. L.; Hartley, J. A.; Hartley, J. M.; Knox, R. J.; McGowan, P. C. Functionalised cyclopentadienyl titanium compounds as potential anticancer drugs. *Dalton Trans.* **2007**, 5082–5090.
- (16) Gao, L. M.; Matta, J.; Rheingold, A. L.; Meléndez, E. Synthesis, Structure and Biological Activity of Amide-Functionalized Titanocenyls: Improving their Cytotoxic Properties. *J. Organomet. Chem.* **2009**, *694*, 4134–4139.
- (17) Kaluđerović, G. N.; Tayurskaya, V.; Paschke, R.; Prashar, S.; Fajardo, M.; Gómez-Ruiz, S. Synthesis, characterization and biological studies of alkenyl-substituted titanocene(IV) carboxylate complexes. *Appl. Organomet. Chem.* **2010**, *24*, 656–662.
- (18) Gómez-Ruiz, S.; Kaluđerović, G. N.; Prashar, S.; Polo-Cerón, D.; Fajardo, M.; Žižák, Ž.; Sabo, T. J.; Juranić, Z. D. Cytotoxic studies of substituted titanocene and ansa-titanocene anticancer drugs. *J. Inorg. Biochem.* **2008**, *102*, 1558–1570.
- (19) Gómez-Ruiz, S.; Gallego, B.; Žižák, Ž.; Hey-Hawkins, E.; Juranić, Z. D.; Kaluđerović, G. N. Titanium(IV) carboxylate complexes: Synthesis, structural characterization and cytotoxic activity. *Polyhedron* **2010**, *29*, 354–360.
- (20) Fichtner, I.; Pampillón, C.; Sweeney, N. J.; Strohfeldt, K.; Tacke, M. Anti-tumor activity of Titanocene Y in xenografted Caki-1 tumors in mice. *Anti-Cancer Drugs* **2006**, *17*, 333–336.
- (21) Lally, G.; Deally, A.; Hackenberg, F.; Quinn, S. J.; Tacke, M. Titanocene Y - Transport and Targeting of an Anticancer Drug Candidate. *Lett. Drug Des. Discovery* **2013**, *10*, 675–682.
- (22) Lord, R. M.; Mannion, J. J.; Crossley, B. D.; Hebden, A. J.; McMullon, M. W.; Fisher, J.; Phillips, R. M.; McGowan, P. C. β -Diketonato Titanium Compounds Exhibiting High In Vitro Activity and Specific DNA Base Binding. *ChemistrySelect* **2016**, *1*, 6598–6605.
- (23) Manna, C. M.; Armony, G.; Tshuva, E. Y. Unexpected Influence of Stereochemistry on the Cytotoxicity of Highly Efficient TiIV Salan Complexes: New Mechanistic Insights. *Chem. - Eur. J.* **2011**, *17*, 14094–14103.
- (24) Miller, M.; Braithwaite, O.; Hochman, J.; Tshuva, E. Y. Insights into molecular mechanism of action of salan titanium(IV) complex with in vitro and in vivo anticancer activity. *J. Inorg. Biochem.* **2016**, *163*, 250–257.
- (25) Cini, M.; Bradshaw, T. D.; Woodward, S. Using titanium complexes to defeat cancer: the view from the shoulders of titans. *Chem. Soc. Rev.* **2017**, *46*, 1040–1051.
- (26) Shavit, M.; Peri, D.; Manna, C. M.; Alexander, J. S.; Tshuva, E. Y. Active Cytotoxic Reagents Based on Non-metallocene Non-diketonato Well-Defined C₂-Symmetrical Titanium Complexes of Tetradentate Bis(phenolato) Ligands. *J. Am. Chem. Soc.* **2007**, *129*, 12098–12099.
- (27) Immel, T. A.; Grutzke, M.; Spate, A.-K.; Groth, U.; Ohlschlager, P.; Huhn, T. Synthesis and X-ray structure analysis of a heptacoordinate titanium(IV)-bis-chelate with enhanced in vivo antitumor efficacy. *Chem. Commun.* **2012**, *48*, 5790–5792.
- (28) Severin, G. W.; Nielsen, C. H.; Jensen, A. I.; Fonslet, J.; Kjær, A.; Zhuravlev, F. Bringing Radiotracing to Titanium-Based Antineoplastics: Solid Phase Radiosynthesis, PET and ex Vivo Evaluation of Antitumor Agent [45Ti](salan)Ti(dipic). *J. Med. Chem.* **2015**, *58*, 7591–7595.
- (29) Tinoco, A. D.; Saxena, M.; Sharma, S.; Noinaj, N.; Delgado, Y.; Quiñones González, E. P.; Conklin, S. E.; Zambrana, N.; Loza-Rosas, S. A.; Parks, T. B. Unusual Synergism of Transferrin and Citrate in the Regulation of Ti(IV) Speciation, Transport, and Toxicity. *J. Am. Chem. Soc.* **2016**, *138*, 5659–5665.

- (30) Keer, H. N.; Kozlowski, J. M.; Tsai, Y. C.; Lee, C.; McEwan, R. N.; Grayhack, J. T. Elevated transferrin receptor content in human prostate cancer cell lines assessed in vitro and in vivo. *J. Urol.* **1990**, *143*, 381–385.
- (31) Weinberg, R. *The biology of cancer*; Garland Science: New York, 2013; p 960.
- (32) Buss, J. L.; Torti, F. M.; Torti, S. V. The role of iron chelation in cancer therapy. *Curr. Med. Chem.* **2003**, *10*, 1021–1034.
- (33) Chong, H.-S.; Ma, X.; Lee, H.; Bui, P.; Song, H. A.; Birch, N. Synthesis and Evaluation of Novel Polyaminocarboxylate-Based Antitumor Agents. *J. Med. Chem.* **2008**, *51*, 2208–2215.
- (34) Yu, Y.; Gutierrez, E.; Kovacevic, Z.; Saletta, F.; Obeid, P.; Suryo Rahmanto, Y.; R. Richardson, D. Iron Chelators for the Treatment of Cancer. *Curr. Med. Chem.* **2012**, *19*, 2689–2702.
- (35) Parks, T. B.; Cruz, Y. M.; Tinoco, A. D. Applying the Fe(III) Binding Property of a Chemical Transferrin Mimetic to Ti(IV) Anticancer Drug Design. *Inorg. Chem.* **2014**, *53*, 1743–1749.
- (36) Cappellini, M. D. Exjade® (deferasirox, ICL670) in the treatment of chronic iron overload associated with blood transfusion. *Ther. Clin. Risk Manag.* **2007**, *3*, 291–299.
- (37) Steinhauser, S.; Heinz, U.; Bartholomä, M.; Weyhermüller, T.; Nick, H.; Hegetschweiler, K. Complex Formation of ICL670 and Related Ligands with FeIII and FeII. *Eur. J. Inorg. Chem.* **2004**, *2004*, 4177–4192.
- (38) Crispioni, G.; Nurchi, V. M.; Crespo-Alonso, M.; Sanna, G.; Zoroddu, M. A.; Alberti, G.; Biesuz, R. A Speciation Study on the Perturbing Effects of Iron Chelators on the Homeostasis of Essential Metal Ions. *PLoS One* **2015**, *10*, e0133050.
- (39) Chantrel-Groussard, K.; Gaboriau, F.; Pasdeloup, N.; Havouis, R.; Nick, H.; Pierre, J.-L.; Brissot, P.; Lescoat, G. The new orally active iron chelator ICL670A exhibits a higher antiproliferative effect in human hepatocyte cultures than O-trenox. *Eur. J. Pharmacol.* **2006**, *541*, 129–137.
- (40) Shanta, S. R.; Kim, T. Y.; Hong, J. H.; Lee, J. H.; Shin, C. Y.; Kim, K. H.; Kim, Y. H.; Kim, S. K.; Kim, K. P. A new combination MALDI matrix for small molecule analysis: application to imaging mass spectrometry for drugs and metabolites. *Analyst* **2012**, *137*, 5757–62.
- (41) Sheldrick, G. Crystal structure refinement with SHELXL. *Acta Crystallogr., Sect. C: Struct. Chem.* **2015**, *71*, 3–8.
- (42) Dolomanov, O. V.; Bourhis, L. J.; Gildea, R. J.; Howard, J. A. K.; Puschmann, H. OLEX2: a complete structure solution, refinement and analysis program. *J. Appl. Crystallogr.* **2009**, *42*, 339–341.
- (43) Kruger, N. J. The Bradford Method for Protein Quantitation. In *Basic Protein and Peptide Protocols*; Walker, J. M., Ed.; Humana Press: Totowa, NJ, 1994; Vol. 32, pp 9–15.
- (44) Schlabach, M. R.; Bates, G. W. The synergistic binding of anions and Fe³⁺ by transferrin. Implications for the interlocking sites hypothesis. *J. Biol. Chem.* **1975**, *250*, 2182–2188.
- (45) Shannon, R. D. Revised effective ionic radii and systematic studies of interatomic distances in halides and chalcogenides. *Acta Crystallogr., Sect. A: Cryst. Phys., Diff., Theor. Gen. Crystallogr.* **1976**, *32*, 751–767.
- (46) Tshuva, E. Y.; Ashenhurst, J. A. Cytotoxic Titanium(IV) Complexes: Renaissance. *Eur. J. Inorg. Chem.* **2009**, *2009*, 2203–2218.
- (47) Go, Y.-M.; Jones, D. P. The Redox Proteome. *J. Biol. Chem.* **2013**, *288*, 26512–26520.
- (48) Tinoco, A. D.; Eames, E. V.; Valentine, A. M. Reconsideration of Serum Ti(IV) Transport: Albumin and Transferrin Trafficking of Ti(IV) and Its Complexes. *J. Am. Chem. Soc.* **2008**, *130*, 2262–2270.
- (49) Parker Siburt, C. J.; Lin, E. M.; Brandt, S. J.; Tinoco, A. D.; Valentine, A. M.; Crumbliss, A. L. Redox potentials of Ti(IV) and Fe(III) complexes provide insights into titanium biodistribution mechanisms. *J. Inorg. Biochem.* **2010**, *104*, 1006–1009.
- (50) Tinoco, A. D.; Thomas, H. R.; Incarvito, C. D.; Saghatelyan, A.; Valentine, A. M. Cytotoxicity of a Ti(IV) compound is independent of serum proteins. *Proc. Natl. Acad. Sci. U. S. A.* **2012**, *109*, 5016–5021.
- (51) Meker, S.; Braithwaite, O.; Hall, M. D.; Hochman, J.; Tshuva, E. Y. Specific Design of Titanium(IV) Phenolato Chelates Yields Stable and Accessible, Effective and Selective Anticancer Agents. *Chem. - Eur. J.* **2016**, *22*, 9986–9995.
- (52) Baramov, T.; Keijzer, K.; Irran, E.; Mosker, E.; Baik, M. H.; Süssmuth, R. Synthesis and Structural Characterization of Hexacoordinate Silicon, Germanium, and Titanium Complexes of the E-coli Siderophore Enterobactin. *Chem. - Eur. J.* **2013**, *19*, 10536–10542.
- (53) Jones, K. E.; Batchler, K. L.; Zalouk, C.; Valentine, A. M. Ti(IV) and the Siderophore Desferrioxamine B: A Tight Complex Has Biological and Environmental Implications. *Inorg. Chem.* **2017**, *56*, 1264–1272.
- (54) Jeon, S.-R.; Lee, J.-W.; Jang, P.-S.; Chung, N.-G.; Cho, B.; Jeong, D.-C. Anti-leukemic properties of deferasirox via apoptosis in murine leukemia cell lines. *Blood Res.* **2015**, *50*, 33–39.
- (55) Theerasilp, M.; Chalermpanapun, P.; Ponlamuangdee, K.; Sukvanitvichai, D.; Nasongkla, N. Imidazole-modified deferasirox encapsulated polymeric micelles as pH-responsive iron-chelating nanocarrier for cancer chemotherapy. *RSC Adv.* **2017**, *7*, 11158–11169.
- (56) Diaz-Garcia, J. D.; Gallegos-Villalobos, A.; Gonzalez-Espinoza, L.; Sanchez-Nino, M. D.; Villarrubia, J.; Ortiz, A. Deferasirox nephrotoxicity—the knowns and unknowns. *Nat. Rev. Nephrol.* **2014**, *10*, 574–586.
- (57) Shavit, M.; Peri, D.; Melman, A.; Tshuva, E. Y. Antitumor reactivity of non-metallocene titanium complexes of oxygen-based ligands: is ligand lability essential? *JBIC, J. Biol. Inorg. Chem.* **2007**, *12*, 825–30.
- (58) Levina, A.; Crans, D. C.; Lay, P. A. Speciation of metal drugs, supplements and toxins in media and bodily fluids controls in vitro activities. *Coord. Chem. Rev.* **2017**, DOI: [10.1016/j.ccr.2017.01.002](https://doi.org/10.1016/j.ccr.2017.01.002).
- (59) Schur, J.; Manna, C. M.; Deally, A.; Koster, R. W.; Tacke, M.; Tshuva, E. Y.; Ott, I. A comparative chemical-biological evaluation of titanium(iv) complexes with a salan or cyclopentadienyl ligand. *Chem. Commun.* **2013**, *49*, 4785–4787.
- (60) Peters, T., Jr. *All about albumin: Biochemistry, genetics, and medical applications*; Academic Press: San Diego, CA, 1996.
- (61) Peri, D.; Meker, S.; Shavit, M.; Tshuva, E. Y. Synthesis, Characterization, Cytotoxicity, and Hydrolytic Behavior of C2- and C1-Symmetrical TiIV Complexes of Tetradentate Diamine Bis-(Phenolato) Ligands: A New Class of Antitumor Agents. *Chem. - Eur. J.* **2009**, *15*, 2403–2415.
- (62) Bonvin, G.; Bobst, C. E.; Kaltashov, I. A. Interaction of transferrin with non-cognate metals studied by native electrospray ionization mass spectrometry. *Int. J. Mass Spectrom.* **2017**, DOI: [10.1016/j.ijms.2017.01.014](https://doi.org/10.1016/j.ijms.2017.01.014).
- (63) Tinoco, A. D.; Incarvito, C. D.; Valentine, A. M. Calorimetric, Spectroscopic, and Model Studies Provide Insight into the Transport of Ti(IV) by Human Serum Transferrin. *J. Am. Chem. Soc.* **2007**, *129*, 3444–3454.
- (64) Grootveld, M.; Bell, J. D.; Halliwell, B.; Aruoma, O. I.; Bomford, A.; Sadler, P. J. Non-transferrin-bound iron in plasma or serum from patients with idiopathic hemochromatosis—Characterization by high-performance liquid-chromatography and nuclear magnetic resonance spectroscopy. *J. Biol. Chem.* **1989**, *264*, 4417–4422.
- (65) Collins, J. M.; Uppal, R.; Incarvito, C. D.; Valentine, A. M. Titanium(IV) Citrate Speciation and Structure under Environmentally and Biologically Relevant Conditions. *Inorg. Chem.* **2005**, *44*, 3431–3440.
- (66) Bertini, I.; Gray, H. B.; Stiefel, E. I.; Valentine, J. S. *Biological Inorganic Chemistry: Structure and Reactivity*; University Science Books: Mill Valley, CA, 2007.